Studies on Fatigue of Mild Steel by a Corrosion Method.

By

Toshio Nishihara and Minoru Kawamoto.

Abstract.

The fatigued zone in mild steel can be detected by a corrosion method as well as when yielded parts are shown as a strain figure. By the corrosion method, the authors have studied the appearances of the fatigued zone and fatigue crack in each specimen at progressive stages of fatigue. Consideration has also been made of the mechanism of fatigue failure with specimens having a smooth surface and having various notches.

I. Introduction.

It is a well-known fact that the yielded parts in mild steel can be detected as a strain figure by Fly's reagent. The reason for this lies in the fact that yielded parts have little resistance to corrosion owing to the existence of many slip bands in crystals. Similarly in a fatigued zone there are many slip bands in crystals, so that fatigued zones in mild steel should be detected also by a corrosion method as a figure. Therefore, the authors have attempted a study of the mechanism of fatigue failure by the corrosion method.

Researches were made for fatigue at various cyclical stresses; that is, direct, bending (cantilever type and uniform bending moment type) and torsional stresses. Corrosion tests were applied to all the specimens—specimens broken at stresses over the fatigue limit, specimens not yet broken on the way to failure, and specimens not broken at stresses under the fatigue limit,—and fatigued zones and fatigue cracks in these specimens were detected. Consideration was given to the etching figures obtained. It is a matter of course that the mechanisms of fatigue failure are very different according to the forms of the specimens—whether they have a smooth surface or not. Therefore, the contents of this paper can be classified in two parts, that is, the case of specimens with smooth surface and the case of specimens with various notches.

To what section of specimens should corrosion tests be applied? The subject is not always an indisputable matter, especially in the case of specimens with notches, because fatigued zones and cracks are distributed three-dimensionally in such specimens. In the experiments reported in this paper in every case we took the longitudinal sections of specimens for corrosion tests. So that etching figures due to segregation appear linearly in the direction of the longitudinal axis of our specimens. But the figure due to segregation can easily be discriminated from the figure due to fatigue. Generally the discrimination is easier in the longitudinal section than in the cross section.

II. Test Piece Materials.

To detect the figure of fatigued zones clearly, the test piece materials must be dead mild steel. According to our experience all the steels of less than 0.1% carbon content will show distinct figuers of fatigued zones at corrosion tests, if only the treatment is proper. The test piece materials used in these experiments were of the following three kinds of steels:

(1) Swedish low carbon steel received in the form of bars 30 mm in diameter and about 3.5 meters in length. This material is marked "6991FA".

(2) Mild steel received in the form of bars 22 mm in diameter and about 2.5 meters in length. This material is marked "7411".

(3) Mild steel received in the form of bars 25 mm in diameter and about 5.5 meters in length. This material is marked "5637".

Table 1.

Chemical Composition of Materials.

Marks of Materials	C %	Mn %	Si %	P %	S %
6991FA	0.09	0.38	—	0.009	0.025
7411	,,	,,	0.10	0.045	0.038
5637	0.10	0.62	0.16	0.040	0.040

The chemical compositions of these materials are shown in Table 1. The "6991FA" material supplied most of the specimens with smooth surface, but part of those with notches. Both "7411" and "5637" were wholly employed in specimens with notches; the former to rotating bending tests and the latter to reversed torsional tests.

Before making fatigue tests, all the materials were heat-treated as shown in Table 2. Appropriate heat-treatment is an important matter in these experiments, because it not only takes off the initial strain, but also it exerts influence upon the distinctness of the etching figure.

Static tensile tests were made on two specimens of each material. The diameter of the tensile

Table 2.

Heat-Treatment and Mechanical Properties of Materials.

Marks of Materials	Heat-Treatment	Upper Yield Point kg/mm²	Lower Yield Point kg/mm²	Ultimate Strength kg/mm²	Breaking Stress on Final Area kg/mm²	Elongation %	Reduction of Area %	Brinell* Hardness Number
6991FA	900°C, 40 mn, Annealed	31.5	23.3	32.8	87.0	49.9	73.7	83.1
		31.1	24.3	33.2	87.2	56.1	73.9	85.8
7411	900°C, 40 mn, Normalized	31.3	24.5	38.5	86.8	42.7	71.4	119
		32.5	25.6	38.6	85.6	46.7	70.6	114
5637	Ditto	33.0	26.8	40.3	94.6	44.6	72.4	114
		35.2	26.5	40.2	94.4	45.2	72.5	114

Two specimens were tested for every material.
* Load was 3000 kg and ball diameter was 10 mm.

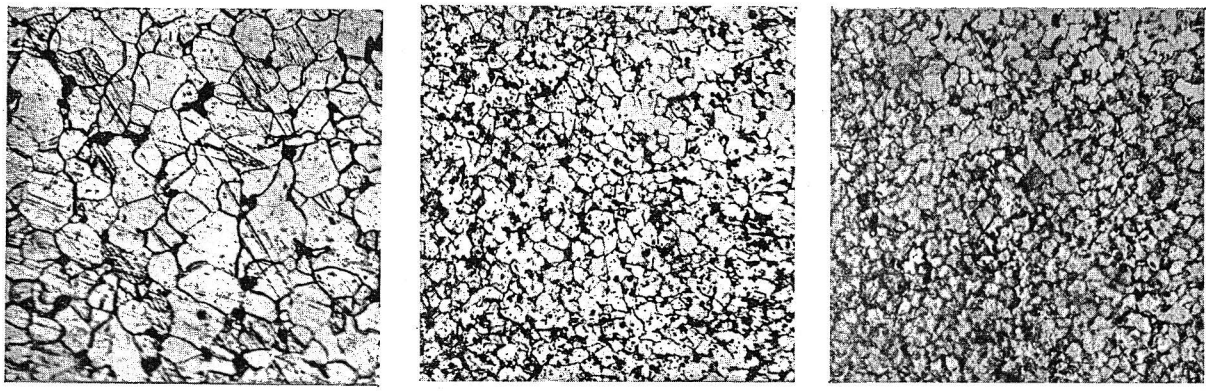

6991FA (Annealed) 7411 (Normalized) 5637 (Normalized)

Fig. 1.

Microscopical Structures of Materials.

specimen was 14 mm and the gauge length was 50 mm. The mechanical properties obtained from the static tensile tests are summarized in Table 2. Also Brinell hardness tests were made and the results are included in Table 2.

Microscopical examination on structure was carried out and photographs obtained are shown in Fig. 1. Attention must be payed to the fact that the "6991FA" material has large grain size and low static strength, but this material showed clear etching figures very rapidly in corrosion tests.

III. Procedure of Experiments.

Specimens were made of the materials thus annealed or normalized, and subjected to fatigue tests. After the fatigue tests, every specimen was tempered at 200°C about 30 minutes in an oil bath, and cooled slowly. This operation is important and must be done with care. After the tempering, specimens were attached to a shaping machine and cut in half longitudinally. The cutting should be made bit by bit, so as not to disturb etching figures of fatigued zones by the cutting strain. The sections of specimens were finely finished with files and sand-paper, and subjected to corrosion tests.

As the etching reagent the following compound was adopted for every specimen.

Copper bichloride :	90 g
Hydrochloric acid :	120 cc
Pure water :	100 cc

When a specimen is dipped in the reagent, the fatigue crack, if it exists, appears first. Then the fatigued zone makes its appearance gradually. The time required to detect the fatigued zone from the beginning of etching is different according not only to the kind of material used, but also to the magnitude of the stress applied at fatigue tests. The "6991FA" material showed etching figures rapidly in a few minutes, while in the other materials ("7411" and "5637") sometimes more than ten hours were required. Generally the lower the stress applied, the longer is the time required to detect etching figures.

IV. Experiments on Specimens with Smooth Surface.

The following four kinds of fatigue tests were made on specimens with smooth surface :

(a) Rotating bending tests of cantilever type.

(b) Rotating bending tests of uniform bending moment type.
(c) Reversed torsional tests.
(d) Repeated tension-compression tests.

The "6991FA" material was used for all tests under the annealed condition.

1. *Results of Experiments.*

(a) Rotating bending tests of cantilever type.

Rotating bending tests were carried out with a Wöhler's type testing machine. The form and dimensions of the specimens employed are shown in Fig. 2. Test results are shown in Table 3.

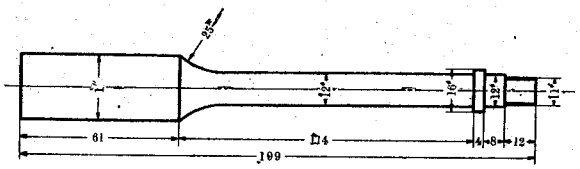

Fig. 2.
Specimen used in Rotating Bending Test of Cantilever Type.

Table 3.
Results of Rotating Bending Tests of Cantilever Type.

Mark of Specimen	Maximum Bending Stress, σ kg/mm²	Number of Repetitions, N in 10^6	Remarks
W–1A	21.5	0.530	Broken
„ 1B	„	0.447	Stopped
„ 1C	„	0.298	„
„ 1D	„	0.149	„
„ 1E	„	0.080	„
„ 1F	„	0.020	„
„ 2	20.0	2.44	Broken
„ 3	19.0	5.86	„
„ 4	18.4	10.42	Unbroken (Fatigue Limit)
„ 5	16.9	10.24	Unbroken

The fatigue limit was 18.4 kg/mm². Under a bending stress of 21.5 kg/mm², specimens at various steps of stress repetitions on the way to failure were subjected to corrosion tests. Marks of specimens in this paper have the following meaning:

The letter before a hyphen shows the kind of fatigue tests.
The first numerical letter after the hyphen shows the magnitude of cyclical stress applied. The higher the number, the lower is the applied stress. The second letter after the hyphen shows the magnitude of the number of stress repetitions under the same stress. The number of stress repetitions becomes smaller in ABC order.

The stress-endurance curve is shown in Fig. 3.

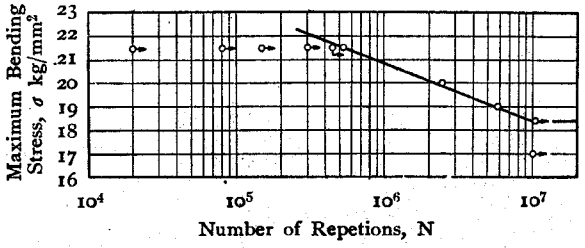

Fig. 3.
Stress-Endurance Curve for Rotating Bending Tests of Cantilever Type.

Etching figures detected on these specimens are shown in Fig. 4. The dark crescent-shaped parts near fillet edges show fatigued zones. In specimen W–2 it is observed that the figure of the fatigued zone is disturbed and partly destroyed by the longitudinal cutting strains.

(b) Rotating bending tests of uniform bending moment type.

Ono's rotating bending testing machine was used for these tests. The form and dimensions of the specimens employed are shown in Fig. 5. The

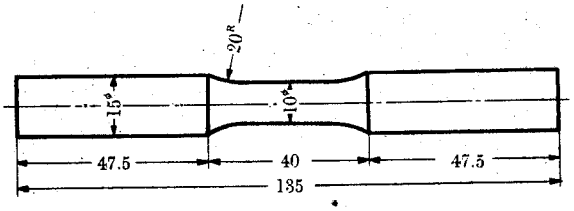

Fig. 5.
Specimen used in Rotating Bending Test of Uniform Bending Moment Type.

Table 4.
Results of Rotating Bending Tests of Uniform Bending Moment Type.

Mark of Specimen	Maximum Bending Stress, τ kg/mm²	Number of Repetitions, N in 10^6	Remarks
O–1	22.04	0.305	Broken
„ 2	21.00	0.460	„
„ 3	19.80	1.388	„
„ 4A	19.05	1.944	„
„ 4B	„	0.700	Stopped
„ 4C	„	0.100	„
„ 5	18.34	12.440	Unbroken (Fatigue Limit)
„ 6	17.00	11.920	Unbroken
„ 7	15.50	10.000	„

test results are shown in Table 4, and the stress-endurance curve in Fig. 6. The fatigue limit in this case is 18.34 kg/mm², which is slightly smaller than that in the preceding case. Etching figures of all the specimens tested are shown in Fig. 7.

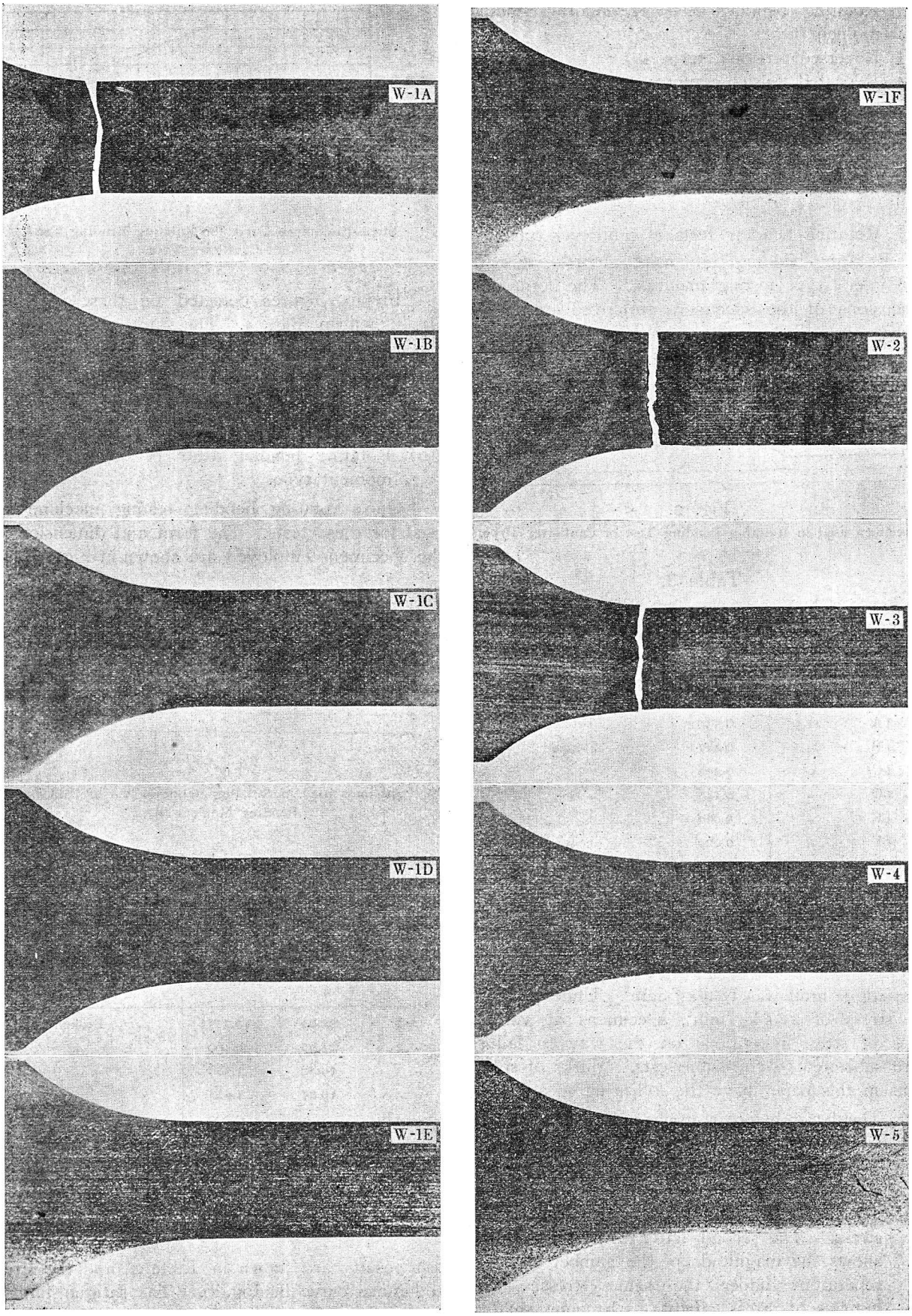

Fig. 4.
Etching Figures on Specimens at Rotating Bending Tests of Cantilever Type.

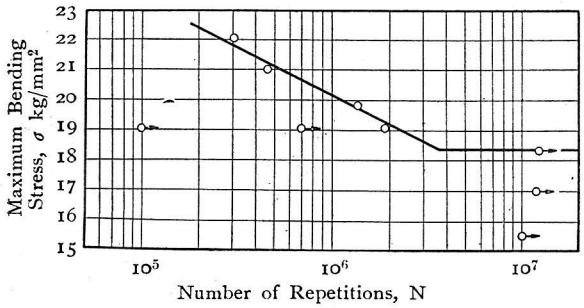

Fig. 6.

Stress-Endurance Curve for Rotating Bending Tests of Uniform Bending Moment Type.

(c) Reversed torsional tests.

Nishihara's reversed torsional testing machine was used for these tests. The form and dimensions of the specimens employed are shown in Fig. 8.

Table 5.

Results of Reversed Torsional Tests.

Mark of Specimen	Maximum Torsional Stress, τ kg/mm²	Number of Repetitions, N in 10^6	Remarks
T-1	11.86	0.614	Broken
„ 2	11.65	0.488	„
„ 3	11.25	0.980	„
„ 4	10.71	2.366	„
„ 5A	10.22	3.976	„
„ 5B	„	1.000	Stopped
„ 5C	„	0.500	„
„ 5D	„	0.100	„
„ 6	10.05	12.082	Broken (Fatigue Limit)
„ 7	9.63	10.434	Unbroken
„ 8	8.49	17.528	„
„ 9	7.50	10.030	„
„ 10	6.48	11.430	„

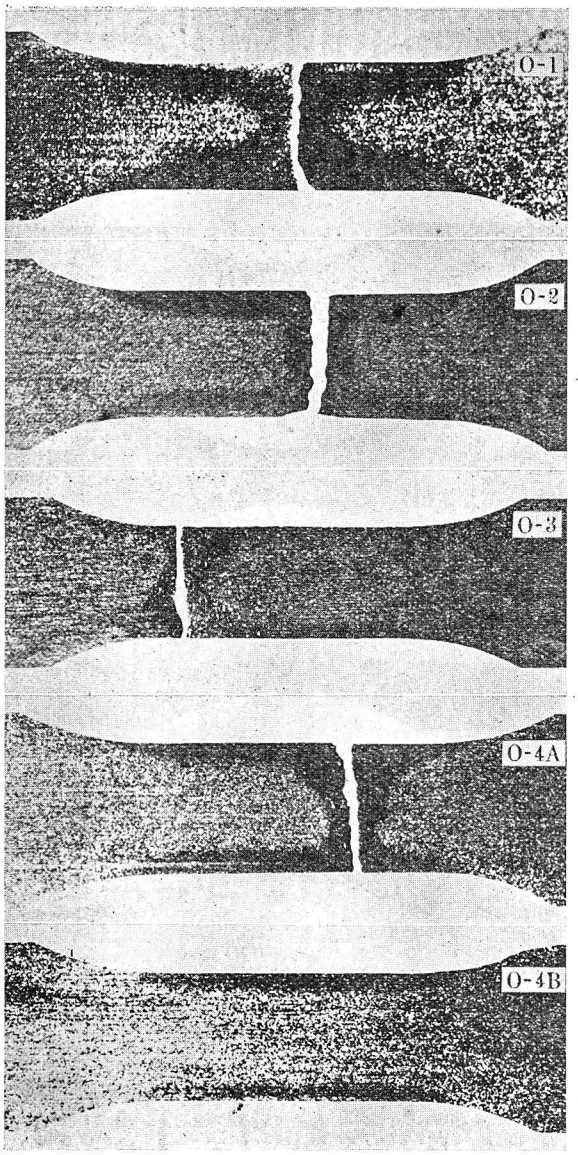

Fig. 7 (1).

Etching Figures at Rotating Bending Tests of Uniform Bending Moment Type.

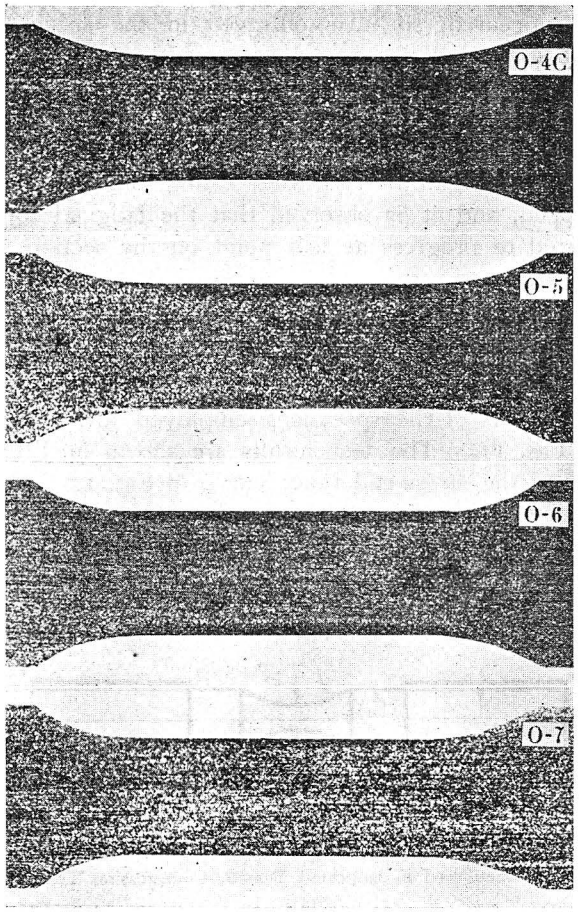

Fig. 7 (2).

Etching Figures at Rotating Bending Tests of Uniform Bending Moment Type.

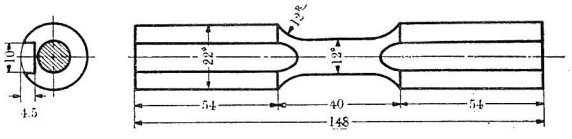

Fig. 8.

Specimen used in Reversed Torsional Test.

Test results are shown in Table 5, and the stress-endurance curve in Fig. 9. Specimen T–6 was broken at stress repetitions of more than 10^7, then we considered the fatigue limit as 10.05 kg/mm^2.

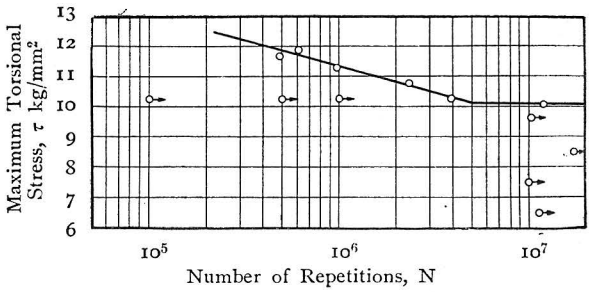

Fig. 9.
Stress-Endurance Curve for Reversed Torsional Tests.

Photographs of etching figures are shown in Fig. 10. At the test of specimen T–4 the testing machine was stopped immediately after a crack had appeared, so it is observed in the specimen that a crack traverses from one side to the other. In specimen T–1 the test was completely carried out, measuring the temperature of the specimen by a thermo-couple. As soon as the temperature of the specimen began to rise, the testing machine was stopped, and it is observed that the fatigued zone started to progress at that point on the section of the specimen.

(d) Repeated tension-compression tests.

Repeated tension-compression tests were carried out with Haigh's testing machine. The form and dimensions of the specimens employed are shown in Fig. 11. The test results are shown in Table 6, and the stress-endurance curve in Fig. 12. The fatigque limit is 15.68 kg/mm^2. Photographs of the etching figures of all the specimens tested are shown in Fig. 13.

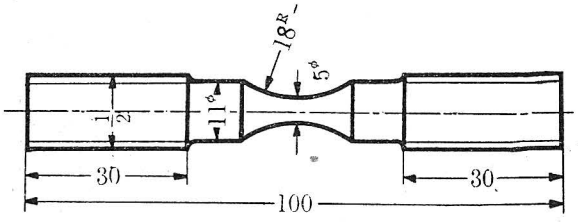

Fig. 11.
Specimen used in Repeated Tension-Compression Test.

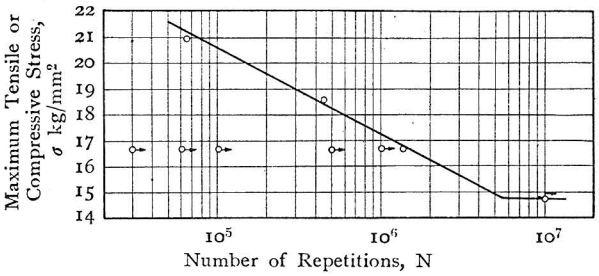

Fig. 12.
Stress-Endurance Curve for Repeated Tension-Compression Tests.

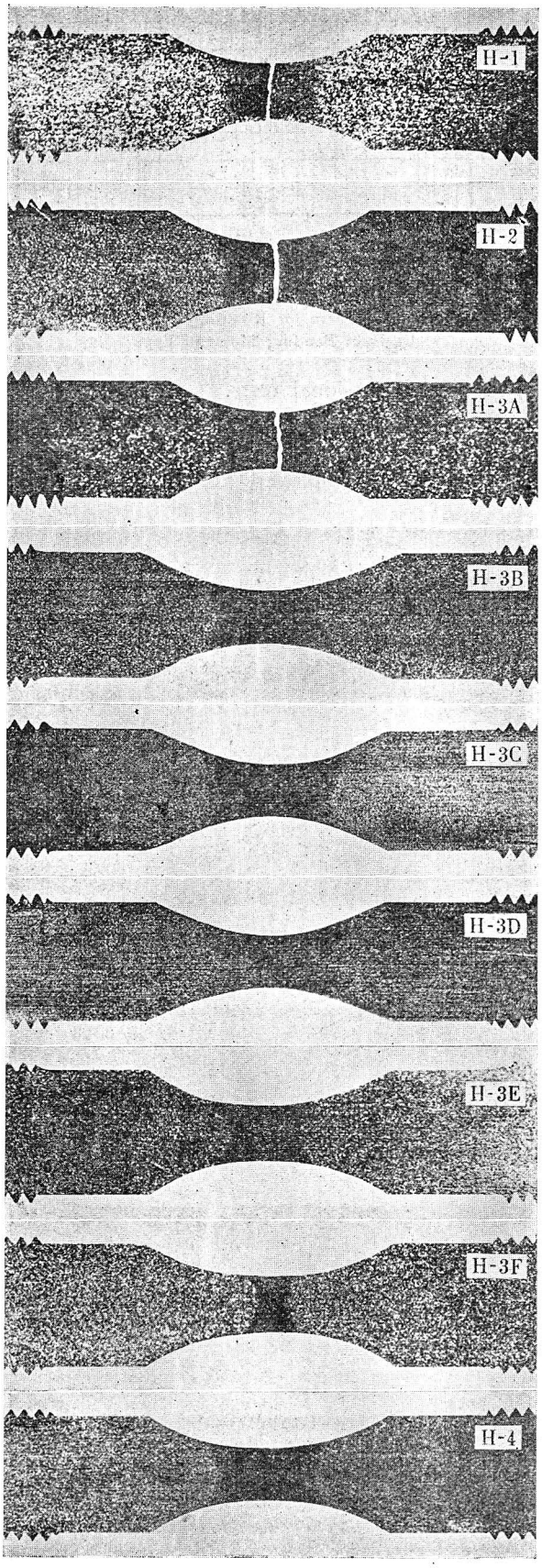

Fig. 13.
Etching Figures on Specimens at Repeated Tension-Compression Tests.

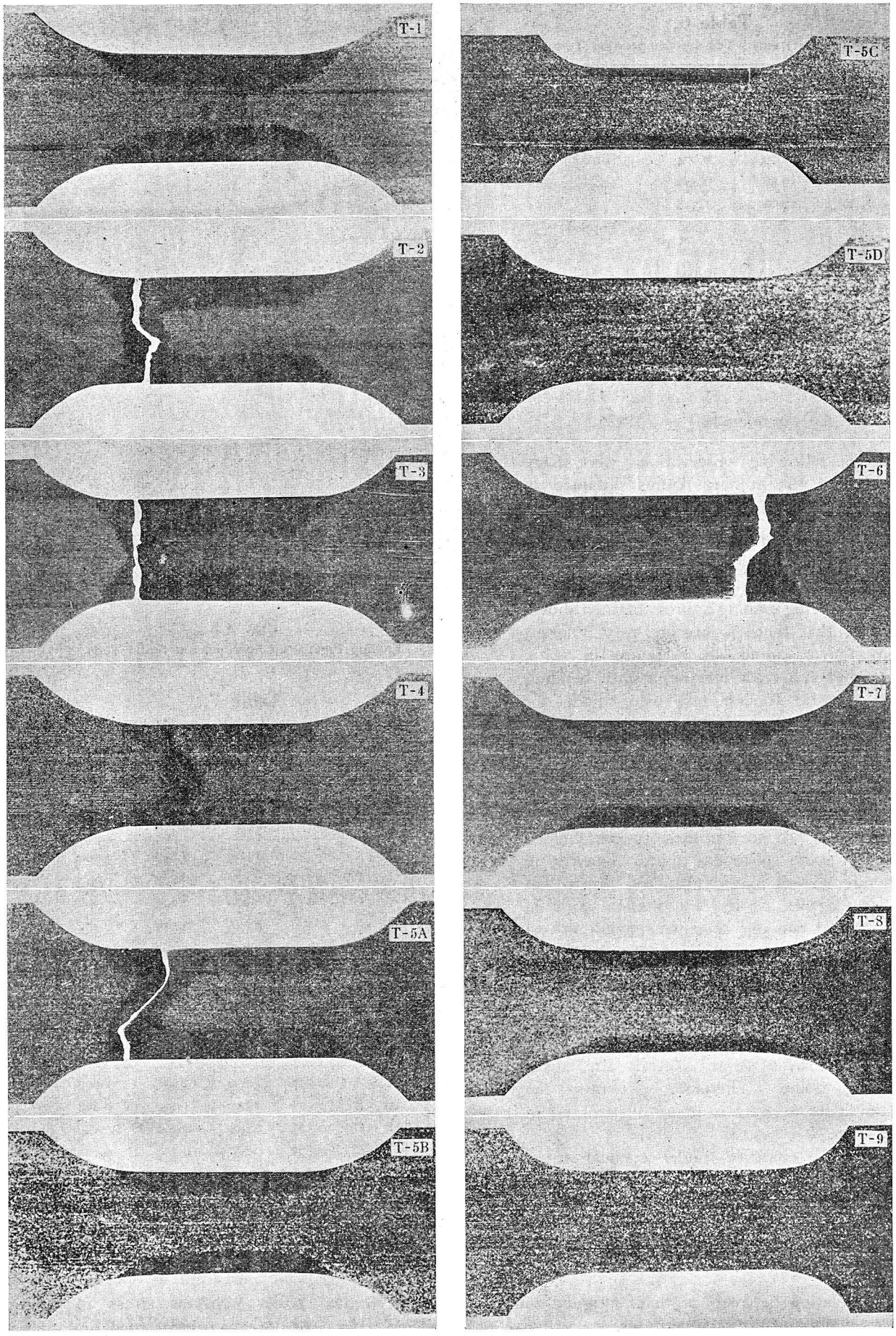

Fig. 10.
Etching Figures on Specimens at Reversed Torsional Tests.

Table 6.

Results of Repeated Tension-Compression Tests.

Mark of Specimen	Maximum Tension-Compression Stress, σ kg/mm^2	Number of Repetitions, N in 10^6	Remarks
H-1	21.99	0.064	Broken
„ 2	19.56	0.442	„
„ 3A	17.66	1.358	„
„ 3B	„	1.000	Stopped
„ 3C	„	0.500	„
„ 3D	„	0.100	„
„ 3E	„	0.060	„
„ 3F	„	0.030	„
„ 4	15.68	10.030	Unbroken (Fatigue Limit)

2. Consideration of Results.

The following observations were made concerning the etching figures obtained in the above-mentioned experiments :—

(a) Comparison of the figure of the fatigued zone with that of the statically yielded zone.

Observing etching figures obtained above, we find that these figures are very different from the so-called strain figure in static tests. Then a static tension, a static bending and a static torsion test were made for comparison. The diameter of the tensile specimen was 14 mm and the bending and tortional specimens were the same as shown in Fig. 2 and Fig. 8, respectively. Etching figures of those static specimens are shown in Fig. 14. As seen in these figures, yielded parts in static specimens appear linearly in the direction of maximum shear stress, that is, 45 degrees to the longitudinal axis in tensile and bending specimens, while in torsional specimens the direction is perpendicular to the longitudinal axis. The reason lies in the fact that static yielding is a matter of stability, so crystals on the line of maximum shear stress slip simultaneously, when the static stress exceeds the upper yielding point. Therefore, generally the strain figure appears in many lines mixed in confusion.

On the contrary, under cyclical stress the fatigued zone appears first at the highest stress parts, and progresses gradually to lower stress parts. So we can easily distinguish between the figure due to fatigue and the figure due to statical stress.

(b) Relation between depth of fatigued zone and number of stress repetitions.

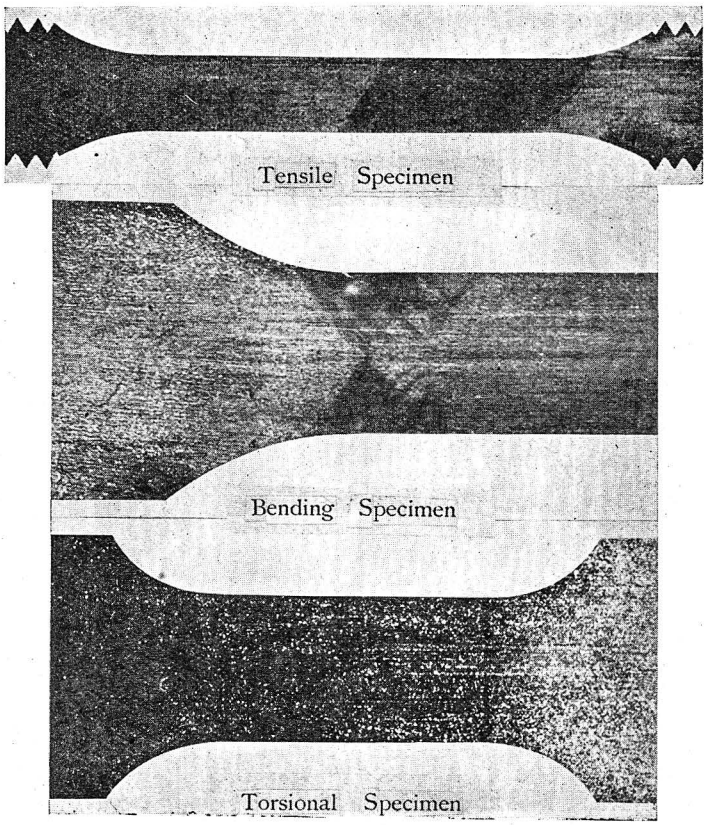

Fig. 14.

Etching Figures on Specimens at Static Tests.

Table 7.

Relation between Depth of Fatigued Zones and the Number of Stress Repetitions.

Kind of Test	Mark of Specimen	a/r	Ratio of a/r, η	Number of Repetitions, N in 10^6	Ratio of Number of Repetitions, ξ	Remarks
Rotating Bending of Cantilever Type	W-1A	0.330	1.000	0.530	1.000	Broken
	„ 1B	0.323	0.979	0.447	0.843	Stopped
	„ 1C	0.299	0.906	0.298	0.562	„
	„ 1D	0.279	0.845	0.149	0.281	„
	„ 1E	0.246	0.745	0.080	0.151	„
	„ 1E	0.100	0.303	0.020	0.038	„
Rotating Bending of Uniform Bending Moment Type	O-4A	0.347	1.000	1.944	1.000	Broken
	„ 4B	0.306	0.882	0.700	0.360	Stopped
	„ 4C	0.187	0.539	0.100	0.051	„
Reversed Torsion	T-5A	0.506	1.000	3.976	1.000	Broken
	„ 5B	0.405	0.800	1.000	0.252	Stopped
	„ 5C	0.333	0.659	0.500	0.126	„
	„ 5D	0.133	0.263	0.100	0.025	„

From the test results we may consider the condition of the fatigued zone progression as the number of stress repetitions increases. Depths of fatigued zones were measured in specimens which were fatigued under constant stress in rotating bending tests (of both cantilever type and uniform

bending moment type) and in reversed torsional tests.

Let a=depth of the fatigued zone
r=radius of the specimen

The value of a in broken specimens of rotating bending tests of uniform bending moment type and reversed torsional tests was measured at a point far from the failure point. Then the value of a/r was calculated for each specimen, as shown in Table 7. Fig. 15 shows the relation between a/r and the

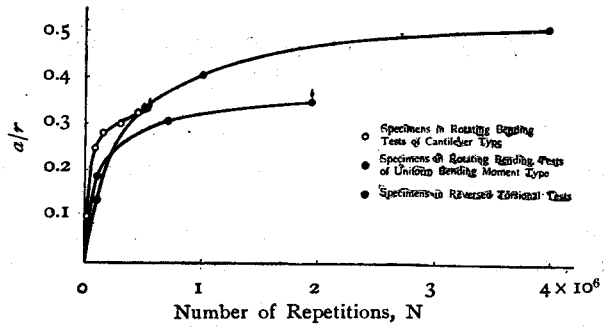

Fig. 15.
Relation between Depth of Fatigued Zone and Number of Repetitions in Smooth Specimen.

number of stress repetitions in a diagram. In rotating bending tests of cantilever type the value of a/r for broken specimens was deduced from the curve in Fig. 15. As seen in Fig. 15, the progression of the fatigued zone is very rapid at the beginning of stress repetitions and becomes slow gradually.

$$\text{Let } \xi = \frac{\text{number of stress repetitions}}{\text{number of stress repetitions to failure}}$$

$$\eta = \frac{a/r}{a/r \text{ for broken specimen}}$$

Values of ξ and η for each specimen are added in Table 7. The relation between ξ and η is shown in Fig. 16. As seen in this figure, the relation

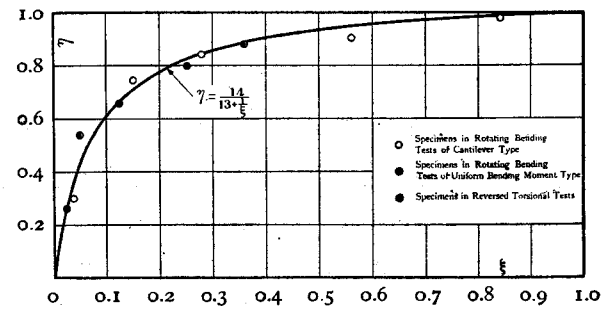

Fig. 16.
Relation between ξ and η.

between ξ and η is determined independently of kinds of tests and also of magnitude of stresses. The curve shown in Fig. 16 is calculated from the following equation:

$$\eta = \frac{14}{13 + \frac{1}{\xi}} \qquad (1)$$

This equations is in good agreement with test results.

The above-mentioned data concerns cases of rotating bending and reversed torsion; that is, cases in which stress distributions is not uniform. But in cases of repeated tension-compression tests the fatigued zone spreads all over the cross section from about 2% of stress repetitions to failure. And the fatigued zone becomes wider gradually as stress repetitions increase.

(c) Fatigued zone and fatigue crack.

In all the specimens we could never find a fatigue crack anywhere apart from the failed sections. The fatigued zone spreads over the whole cross section only at a point near the failed section. From these results it can be deduced that the fatigue crack grows rapidly, if it appears at all, and destruction always occurs at the point where the crack first appeared. About this subject we shall consider further in the experiments on notched specimens.

(d) Relation between depth of the fatigued zone and magnitude of the cyclical stress applied.

The depth of the fatigued zone a was measured for broken and unbroken specimens in rotating bending tests of uniform bending moment type and in reversed torsional tests. As mentioned in the preceding paragraph, the value a represents the depth of the fatigued zone immediately before destruction. The value of a/r for those specimens was calculated and shown in Table 8. Fig. 17 (1) and (2) show the relation between a/r and the magnitude of stresses in a diagram. As seen in these figures, the value of a/r immediately before destruction becomes larger as the applied stress increases.

Table 8.

The Relation between the Depth of Fatigued Zone and the Magnitude of Cyclical Stress Applied.

(1) Rotating Bending Tests of Uniform Bending Moment Type.

Mark of Specimen	a/r	Maximum Bending Stress, σ kg/mm²	Maximum Bending Stress / Fatigue Limit	Remarks
O-1	0.600	22.04	1.202	Broken
„ 2	0.458	21.00	1.145	„
„ 3	0.375	19.80	1.080	„
„ 4A	0.347	19.05	1.039	„
„ 5	0.239	18.34	1.000	Unbroken (Fatigue Limit)
„ 6	0.196	17.00	0.927	Unbroken
„ 7	0.090	15.50	0.845	„

(2) Reversed Torsional Tests.

Mark of Specimen	a/r	Maximum Torsional Stress, τ kg/mm²	Maximum Torsional Stress / Fatigue Limit	Remarks
T–1	0.619	11.86	1.180	Broken
„ 2	0.598	11.65	1.159	„
„ 3	0.661	11.25	1.119	„
„ 4	0.534	10.71	1.066	„
„ 5A	0.506	10.22	1.017	„
„ 6	0.540	10.05	1.000	Broken (Fatigue Limit)
„ 7	0.516	9.63	0.958	Unbroken
„ 8	0.357	8.49	0.845	„
„ 9	0	7.50	0.746	„
„ 10	0	6.48	0.645	„

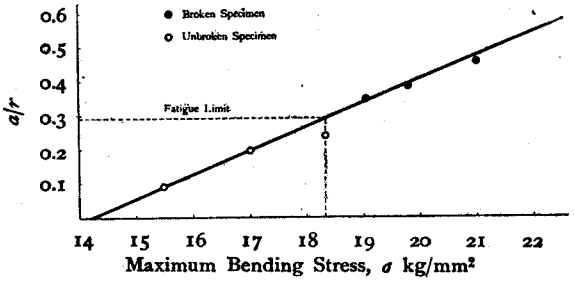

Fig. 17 (1).

Relation between a/r and σ for Rotating Bending Tests of Uniform Bending Moment Type.

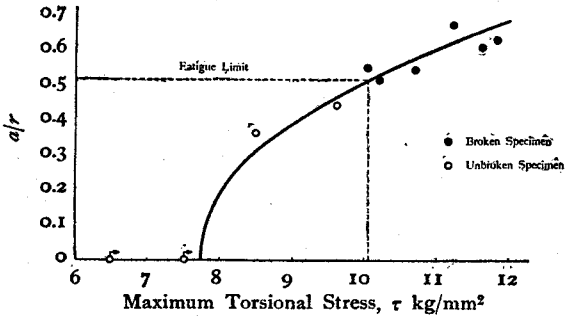

Fig. 17 (2).

Relation between a/r and τ for Reversed Torsional Tests.

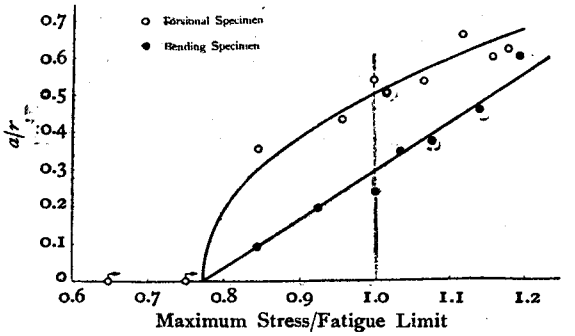

Fig. 18.

Relation between Depth of Fatigue Zone Magnitude of Stress in Smooth Specimens.

It must be particularly noted that the value of a/r is not zero even when the applied stress is under the fatigue limit. That is, the specimen is not broken in spite of the appearance of the fatigued zone at a stress slightly under the fatigue limit. Values of ratios of applied stresses to the fatigue limit are added in Table 7. The relation between values of these ratios and a/r are shown in Fig. 18. The minimum value of the ratio, under which the fatigued zone appears, is equal to 0.77 independently of the kind of stress applied.

V. Experiments on Specimens with Various Notches.

When a crack appears in a specimen with smooth surface, great stress concentration occurs there. Therefore the crack grows very rapidly and leads to destruction in a short time. While in specimens with notches the stress concentration exists from the beginning of the test, so that we can suppose that the crack grows gradually. To ascertain this supposition we made preliminary experiments; that is, reversed torsional tests on the specimen with a key way, as shown in Fig. 19.

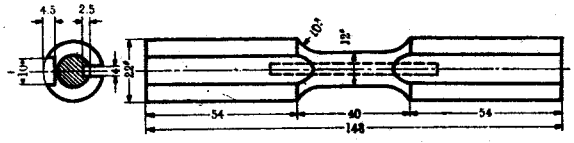

Fig. 19.

Specimen with Key Way.

Table 9.

Results of Reversed Torsional Tests on Specimens with a Key Way.

Mark of Specimen	Maximum Torsional Stress, τ kg/mm²	Number of Repetitions, N in 10^6	Remarks
TK–1	8.65	0.666	Broken
„ 2	7.93	1.792	„
„ 3	7.05	2.453	„
„ 4	6.36	7.444	„
„ 5	5.91	16.190	Unbroken (Fatigue Limit)
„ 6	4.60	13.796	„

The material of the test piece was "6991FA". Test results and the stress-endurance curve are shown in Table 9 and Fig. 20, respectively. An example of the etching figures detected in those specimens is shown in Fig. 21, which shows the section of specimen TK–3 through the center of the key way. We can see many fatigue cracks in the specimen at places far from and near the failure point. So the etching figure gives the appearance of a network, which is very different from that in

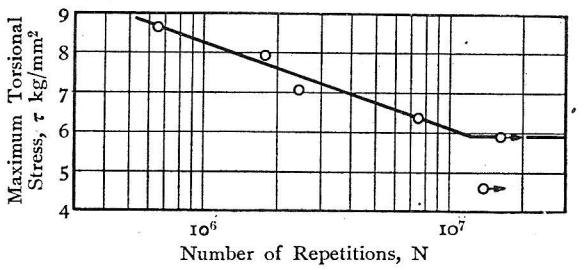

Fig. 20.
Stress-Endurance Curve for Specimens with Key Way.

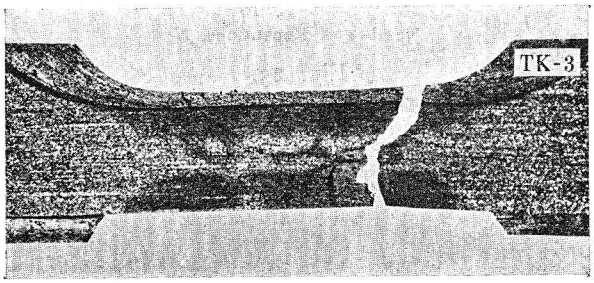

Fig. 21.
Etching Figure on Specimen with Key Way.

6 were reversed torsional tests with Nishihara's fatigue testing machine. As forms of notches in these experiments, we adopted the annular V- or U-shape, because the specimen with the key way, as in Fig. 19, is difficult for accurate machining and also for measurement. Forms of notches on all the specimens were examined by a projecting machine at about 50 magnifications, and special attention was payed to uniformity in the form of notches.

It must be noticed that the stress values in notched specimens in this paper are always the nominal values which are calculated at the bottom of the notches, regardless of the stress concentration.

1. *Experiment–1 : Rotating Bending Tests on the Specimen with Three U-shaped Notches.*

The form and dimensions of the specimens employed are shown in Fig. 22, and results of fatigue tests in Table 11. Diameters of specimens at the bottom of the three notches are also added in Table 11. As seen in the table, the difference between diameters

Table 10.

Kinds of Experiments on Notched Specimens.

No. of Experiment	Kind of Test	Materials Used	Mark of Specimen	Form of Specimen
Experiment–1	Rotating Bending	6991FA	O3U	Specimen with Three U-shaped Notches
„ 2	„	7411	OU	Specimen with a U-shaped Notch of Various Fillet Radius
„ 3	„	„	OV	Specimen with a V-shaped Notch
„ 4	„	„	ODV	Specimen with a Deep and Sharp V-shaped Notch
„ 5	Reversed Torsion	5637	TV	Specimen with a V-shaped Notch
„ 6	„	„	TDV	Specimen with a Deep and Sharp V-shaped Notch

the case of specimens with smooth surface.

Then to investigate the conditions of progression of fatigued zone and fatigue cracks in notched specimens more precisely, we made six kinds of experiments on specimens with various forms of notches, as shown in Table 10. Experiment–1 to Experiment–4 were rotating bending tests of uniform bending moment type, with Ono's fatigue testing machine, and Experiment–5 and Experiment–

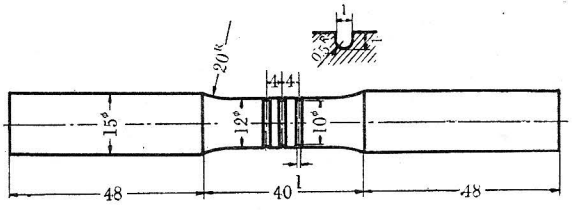

Fig. 22.
Specimen used in Experiment–1.

Table 11.

Results of Fatigue Tests in Experiment–1.

Mark of Specimen	Diameters of Specimen, mm			Maximum Bending Stress, σ kg/mm²	Number of Repetitions, N in 10^6	Remarks
	Left	Middle	Right			
O3U–1	10.00*	10.00	10.00	18.0	0.030	Broken
„ 2	9.98	9.98	9.97*	17.0	0.036	„
„ 3	9.98	9.98	9.99*	16.0	0.065	„
„ 4	9.80*	10.00	9.80	14.5	0.106	„
„ 5	9.83	9.78	9.86*	14.0	0.201	„
„ 6	9.80	9.70	9.80*	13.0	0.492	„
„ 7	9.78*	9.75	9.80	11.0	0.832	„
„ 8	9.96*	9.97	9.97	10.3	1.296	„
„ 9	10.00	10.00	10.00*	9.8	3.771	„
„ 10	9.99	9.99	9.99	9.2	15.999	Unbroken (Fatigue Limit)
„ 11	10.00	10.00	10.00	9.0	10.536	Unbroken

* Shows failed section.

of notches on both sides was always less than 0.03 mm, while the diameter of the middle notch had a considerable difference in each specimen. But this fact causes no trouble in the fatigue test results, because fatigue failure always occurs at the notches on either side, as appears in the later discussion. So the values of the maximum bending stress in Table 11 were calculated on the notches on both side.

Materials used in Experiment–1 were "6991 FA" which was the same as in the experiments of smooth specimens. Therefore, the fatigue test results for this materials with smooth specimens under uniform bending were already shown in

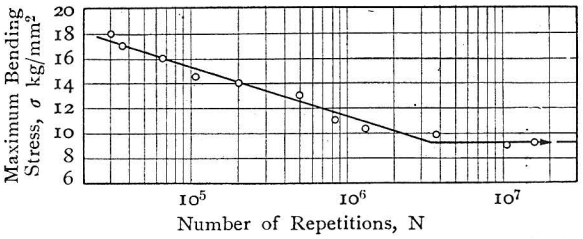

Fig. 23.
Stress-Endurance Curve for Experiment–1.

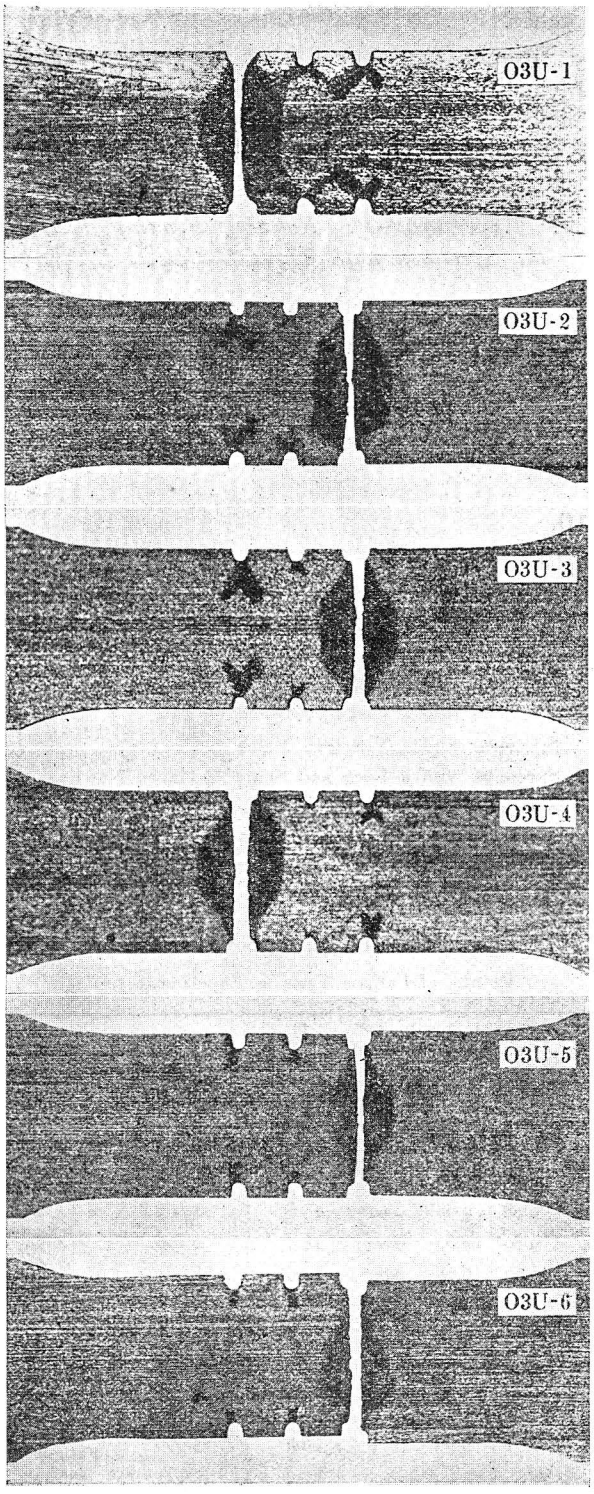

Fig. 24 (1).
Etching Figures in Experiment–1.

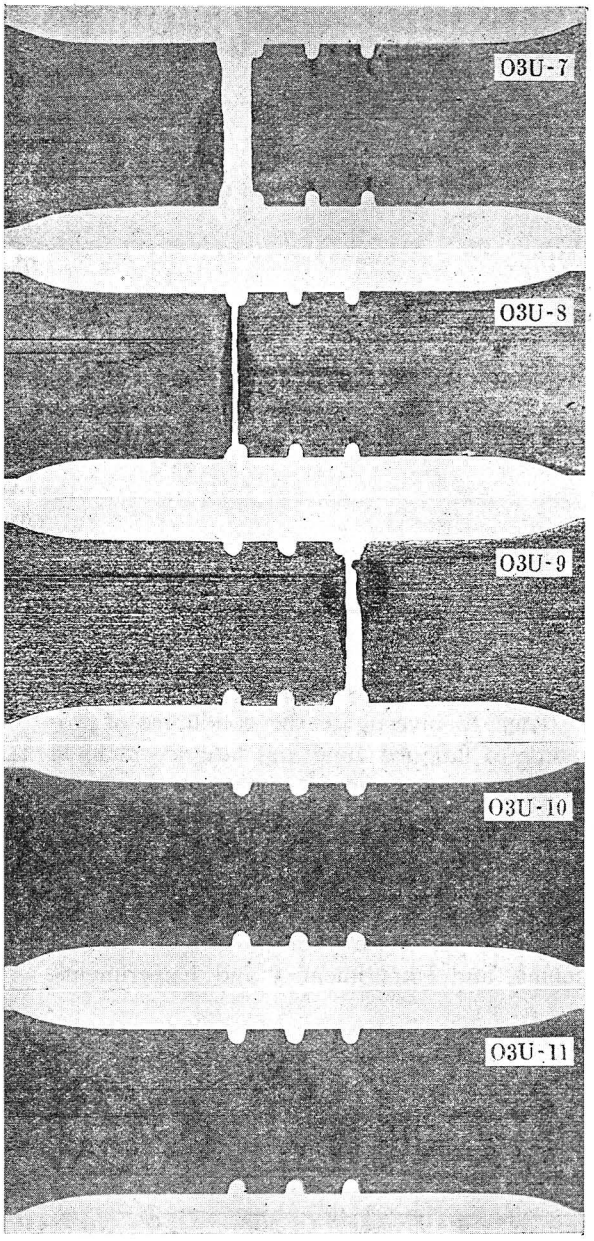

Fig. 24 (2).
Etching Figures in Experiment–1.

Table 4; that is, the fatigue limit was 18.34 kg/mm². While in Experiment–1 the fatigue limit is 9.2 kg/mm² as shown in Table 11. Therefore the coefficient of notch effect for fatigue β is as follows:

$$\beta=\frac{18.3}{9.2}=1.99$$

Fig. 23 shows the stress-endurance curve obtained in Experiment–1.

Photographs of etching figures detected on specimens are shown in Fig. 24. Consideration is made for the etching figures as follows:

(a) Shapes of fatigued zones at unbroken notches.

In all specimens except O3U–9, O3U–10 and O3U–11, we find both fatigued zones and fatigue cracks simultaneously at the bottom of notches not yet broken. This fact suggests that fatigue cracks grow gradually in notched specimens, as expected. We also can see that fatigued zones always appear on both sides of cracks.

Shapes of fatigued zones are very different according to the magnitude of cyclical stress applied. When applied stresses are low, fatigued zones appear thinly on both sides of cracks, and when applied stresses are high, fatigued zones spread linearly in directions inclined at about 45 degrees to the axis of the specimens; that is, in the directions of the maximum shear stress. The higher the applied stress, the longer is the fatigued zone.

As previously mentioned, yielded zones in statically over-stressed specimens appear linearly in the direction of the maximum shear stresses. It thus becomes doubtful whether etching figures on specimens fatigued at high stresses are actually caused by fatigue or not. Therefore, it is very interesting to compare the etching figures detected on fatigued specimens with statical strain figures detected on specimens of the same form. So we applied various values of bending moments statically to the same specimens as shown in Fig. 22. Strain figures obtained are shown in Fig. 25. The nominal values of statical bending stresses σ_n at the bottom of notches were as follows:

For specimen	S3U–1	σ_n=40 kg/mm²
,,	S3U–2	,, 39 ,,
,,	S3U–3	,, 35 ,,
,,	S3U–4	,, 25 ,,

In specimens S3U–1 and S3U–2, the yielded zone appears in many lines at 45 degrees to the longitudinal axis, but the strain figure differs in general appearance from the etching figure on the specimen which was fatigued at the high cyclical stress. In specimens S3U–3 and S3U–4, the yielded zone appears slightly at the bottom of notches, but it does not appear in linear forms under the statical bending stress of those magnitudes. From these results it can be determined that linear-shaped

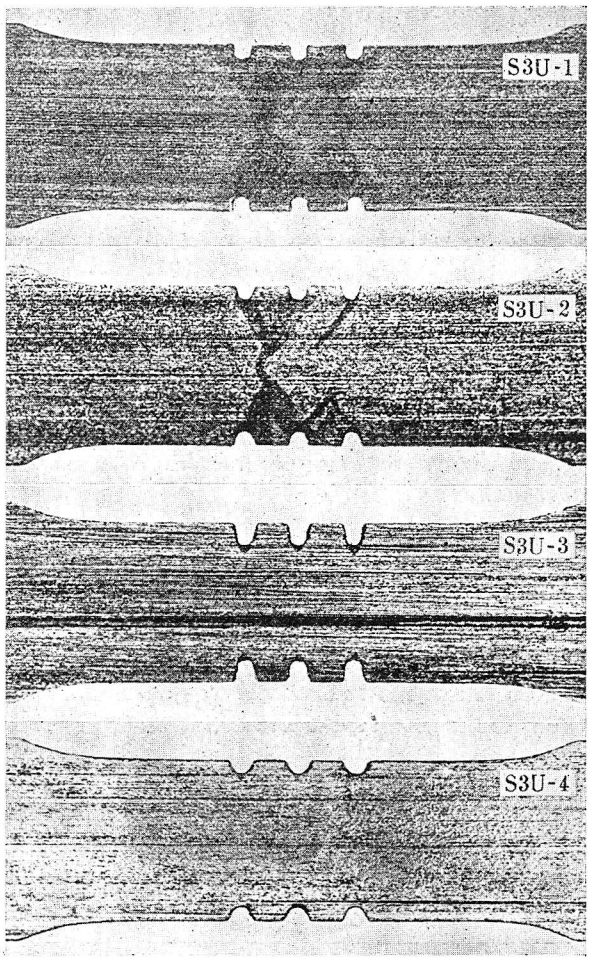

Fig. 25.
Etching Figures on Specimens at Static Bending Tests.

figures on specimens fatigued at high cyclical stresses are not caused by statical stresses, but by fatigue.

(b) Shapes of fatigued zones at broken notches.

In the failed section, the fatigued zone appears narrowly at the bottom of the notch and becomes gradually wider towards the center of the specimen. We can easily understand the reason why the fatigued zone makes this shape, because we know already, in the preceding paragraph, that the fatigued zone appears wider as the stress bocomes higher, and it can be considered that the stress at the bottom tip of the crack becomes higher as the crack progresses.

We are also aware that shapes of fatigued zones at broken notches are different according to the magnitude of the stresses applied. That is, when the applied stress is high, the fatigued zone becomes wider rapidly towards the center of the specimen, and, on the contrary, when the applied stress is low, the fatigued zone becomes wider gradually. So that the area of the fatigued zone becomes smaller as the applied stress becomes lower. This fact is self-evident, for the reason already

mentioned above.

When the applied stress is low, the wide part of the fatigued zone is not always situated at the center of a specimen, but generally leans to one side. Therefore, the shape of the fatigued zone varies according to the section of the specimen which is subjected to fatigue tests. For example, in specimen O3U–8 no wide part appears in the fatigued zone, because the section was taken so as not to pass the wide part. Generally the wide part of the fatigued zone corresponds to the point the fatigue crack progressed very rapidly, and at the point the fatigue fracture appears as a very rough surface. For example, Fig. 26 shows the fatigue fracture of a notched

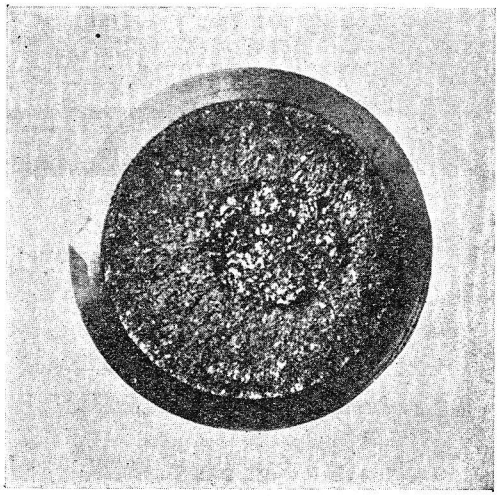

Fig. 26.
Fatigue Fracture of Notched Specimen at Rotating Bending Test.

specimen in a rotating bending test. The ring-shaped part of fine fracture corresponds to the part where the fatigue crack progressed slowly.

(c) Relation between depth of fatigue crack and magnitude of cyclical stress applied.

As seen in Table 11 or Fig. 24, there is no specimen which was broken at the middle notch. In specimen O3U–6, the diameter at the middle notch was considerably smaller than that at the other notches, nevertheless destruction does not occur at the middle notch. The reason lies in the fact that the stress concentration factor at the notch on either side is always greater than the stress concentration factor at the middle notch. Of course, the stress concentration factors at the notches on both sides are equal to each other. Therefore when destruction occurs at the notch on either side, the notch of the other side is considered to be in the state just, or slightly, before destruction.

Then we consider the relation between the magnitude of the stress and the depth of the fatigue crack which is in the state just before destruction.

Let b=depth of the fatigue crack in the state just before destruction
r=radius of the specimen at the bottom of the notch

As the value of b, we took the mean of the two values which are obtained for each specimen in Fig. 24. Calculated values of b/r for all the specimens are shown in Table 12. Fig. 27 shows the

Table 12.
Depth of Fatigue Cracks in Experiment–1.

Mark of Specimen	Maximum Bending Stress, σ kg/mm^2	Maximum Bending Stress / Fatigue Limit	b/r	Remarks
O3U–1	18.0	1.956	0.216	Broken
„ 2	17.0	1.848	0.316	„
„ 3	16.0	1.739	0.362	„
„ 4	14.5	1.576	0.270	„
„ 5	14.0	1.522	0.280	„
„ 6	13.0	1.413	0.234	„
„ 7	11.0	1.196	0.200	„
„ 8	10.3	1.119	0.100	„
„ 9	9.8	1.065	0	„
„ 10	9.2	1.000	0	Unbroken (Fatigue Limit)
„ 11	9.0	0.978	0	Unbroken

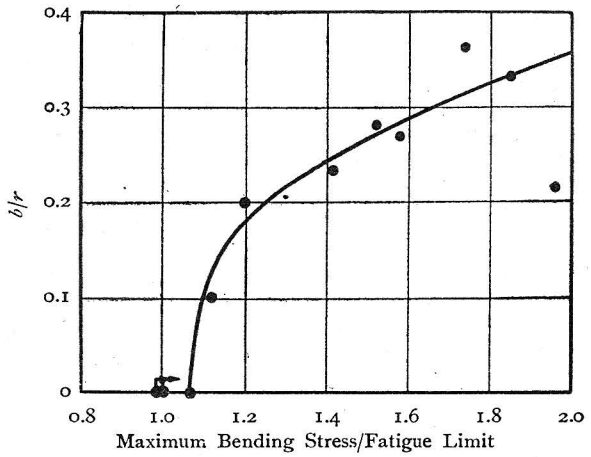

Fig. 27.
Relation between Depth of Cracks and Magnitude of Stress in Experiment–1.

results in a diagram. The relation between b/r and the stress value applied can be expressed approximately by the curve shown in Fig. 26. The higher the applied stress, the larger is the value of b/r.

The relation between b/r and the stress value applied for notched specimens is quite similar to the relation between a/r and the stress value applied for smooth specimens. That is to say, Fig. 26 corresponds to Fig. 18. The principal difference between the two figures is that the intersecting point of the curve with abscissa in Fig. 26 is higher

than the fatigue limit, while that in Fig. 18 was lower than the fatigue limit. For notched specimens fatigue cracks do not appear not only at the fatigue limit, but also at a little more than the fatigue limit, as in the specimen O3U–9. But is must be noted that the question is not the general properties of notched specimens, but the characteristics of Experiment–1. This problem will be fully discussed later, in Experiment–3.

2. *Experiment–2 : Rotating Bending Tests on the Specimen with a U-shaped Notch. The Fillet Radius at the Bottom of the Notch is Varied Stepwise.*

In this experiment we attempted to ascertain how the condition of fatigued-zone or fatigue-crack progression varies as the fillet radius at the bottom of the notch becomes gradually smaller. Specimens employed are shown in Fig. 28 and Fig. 29 (1)~(6). Fig. 28 is a specimen without notches, about

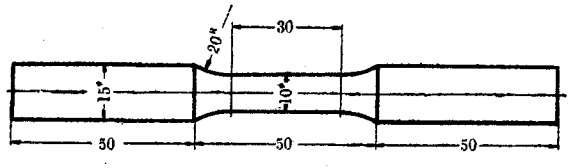

Fig. 28.
Smooth Specimen used in Experiment–2.

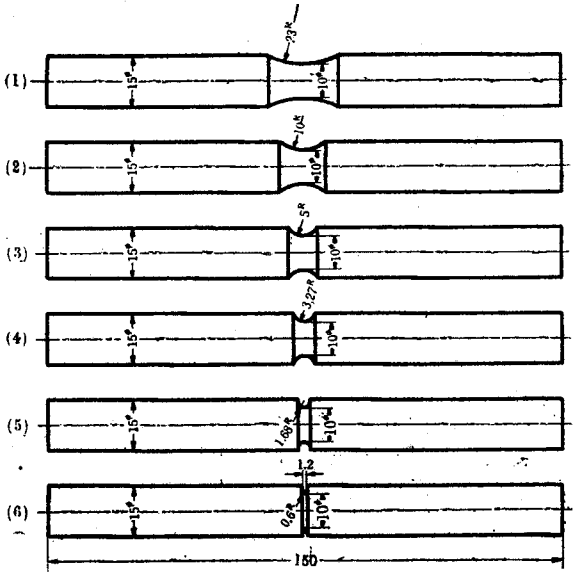

Fig. 29.
Notched Specimens used in Experiment–2.

which the condition of fatigued-zone progression was fully disscussed in IV. So the specimen of Fig. 28 was not subjected to corrosion tests, but used only to determine the fatigue resistance of the "7411" material, and also to compare the fatigue resistance of smooth specimens with that of notched specimens. Fig. 29 shows specimens with U-shaped notches, in which the fillet radius R at the bottom of the notch was varied in six steps, that is, 23, 10, 5, 3.27, 1.68 and 0.6 mm. When the fillet radius R is more than 2.5 mm, the shape of the notch becomes rather a circular arc.

Test results on the smooth specimen of Fig. 28 are shown in Table 13, and the stress-endurance curve in Fig. 30. The fatigue limit was 22.5 kg/mm^2.

Table 13.
Results of Fatigue Tests on Smooth Specimens in Experiment–2.

Mark of Specimen	Maximum Bending Stress, σ kg/mm^2	Number of Repetitions, N in 10^6	Remarks
ON–1	28.0	0.264	Broken
" 2	26.0	1.167(0.860*)	"
" 3	24.5	1.470	"
" 4	23.5	2.720	"
" 5	23.0	7.070	"
" 6	22.5	51.410	Unbroken (Fatigue Limit)
" 7	21.0	20.747	Unbroken

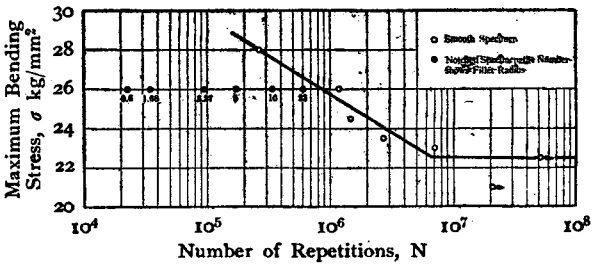

Fig. 30.
Stress-Endurance Curve for Experiment–2.

All the test results on notched specimens in Fig. 29 are summarized in Table 14. The object in Experiment–2 is not to ascertain the fatigue limit of each specimen, but to clear the conditions of fatigued-zone and fatigue-crack progression. We applied the bending stress of 26 kg/mm^2 uniformly to all the specimens. The value of 26 kg/mm^2 was chosen as the stress under which the smooth specimen fails at about 10^6 stress repetitions. Of course, the number of stress repetitions to fracture becomes smaller as the fillet radius R diminishes. As seen in Table 14, the number of stress repetitions to failure was irregular in various specimens. So in considering the results we took the mean value as the number of stress repetitions to fracture. These mean values are shown in Table 14 and also in Fig. 30.

In Experiment–2, corrosion tests were also made on the specimens which were stopped at various steps of stress repetitions on the way to

Table 14.

Results of Fatigue Tests on Notched Specimens in Experiment-2.

Mark of Specimen	Fillet Radius, R mm	Number of Repetitions, N in 10^6	Ratio of Number of Repetitions, ξ	Remarks
OU-1A (1)	23	0.453	1.000	Broken
„ 1A (2)		0.961 mean : 0.602		„
„ 1A (3)		0.393		„
„ 1B		0.300	0.498	Stopped
„ 1C		0.200	0.332	„
„ 1D		0.100	0.166	„
OU-2A (1)	10	0.386	1.000	Broken
„ 2A (2)		0.397 mean : 0.335		„
„ 2A (3)		0.222		„
„ 2B		0.310	0.926	Stopped
„ 2C		0.220	0.657	„
„ 2D		0.100	0.299	„
OU-3A (1)	5	0.201	1.000	Broken
„ 3A (2)		0.144 mean : 0.173		„
„ 3B		0.150	0.867	Stopped
„ 3C		0.100	0.578	„
„ 3D		0.050	0.289	„
OU-4A (1)	3.27	0.831	1.000	Broken
„ 4A (2)		0.1072 mean : 0.0952		„
„ 4B		0.070	0.736	Stopped
„ 4C		0.050	0.525	„
„ 4D		0.010	0.105	„
OU-5A (1)	1.68	0.0383	1.000	Broken
„ 5A (2)		0.0310 mean : 0.0347		„
„ 5B		0.030	0.865	Stopped
„ 5C		0.020	0.577	„
„ 5D		0.010	0.289	„
OU-6A	0.60	0.0225	1.000	Broken
„ 6B		0.0170	0.756	Stopped
„ 6C		0.0113	0.502	„

failure, as in IV. The number of stress repetitions applied to the stopped specimens is also shown in Table 14. Fig. 31 shows the relation between the fillet radius R and the number of stress repetitions in every specimen broken or stopped.

Photographs of etching figures detected on specimens are shown in Fig. 32 (1)~(4). Consideration is made on these etching figures as follows:

(a) Shapes of fatigued zones in stopped specimens.

When the fillet radius R is large, the fatigued zone appears in the shape of a crescent at the bottom of a notch. The reason is self-evident from the fact described previously in IV, *2*, (a); that is, the fatigued zone progresses gradually from high stressed parts to low stressed parts.

It can be seen very clearly in the specimen

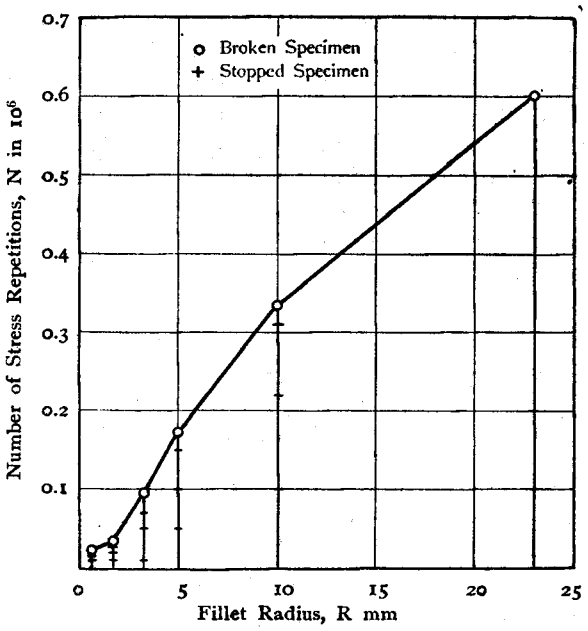

Fig. 31.

Number of Stress Repetitions Applied in Experiment-2.

OU-6B that the fatigued zone appears on both sides of the crack and becomes wider gradually as the crack progresses. As previously mentioned, the fatigued zone spreads in directions inclined at about 45 degrees to the longitudinal axis of the specimen; that is, directions of the maximum shear stress. On the contrary, the fatigue crack develops in the direction of the plane of the maximum principal stress. In specimen OU-5D, the fatigued zone appears in two branches from the first and it suggests the existence of a fatigue crack, though it is small.

(b) Shapes of fatigued zones in broken specimens.

(i) When the fillet radius R is small.

When the fillet radius R is less than 10 mm, the fatigued zone appears wide at the middle part of a specimen. It can be seen in Fig. 32 (2)~(4) that the area of the wide part of the fatigued zone in every broken specimen has a nearly constant magnitude. This fact is very interesting when compared with the result which was already obtained in V, *1*, (b); that is, the area of the fatigued zone becomes smaller as the applied stress becomes lower. From these results it can be deduced that the area of the wide part of the fatigued zone is decided only by the magnitude of the applied stress, and is independent of the value of fillet radius R.

In specimen OU-6A, there appears a linear figure as the statical strain figure. It is certain that the linear figure did not appear in the early stage of the fatigue test, because we can not find the linear figure in specimens stopped before failure. The authors consider that the linear figure happened accidentally by shock at the breaking instant.

(ii) When the fillet radius is large.

When the fillet radius is more than 10 mm,

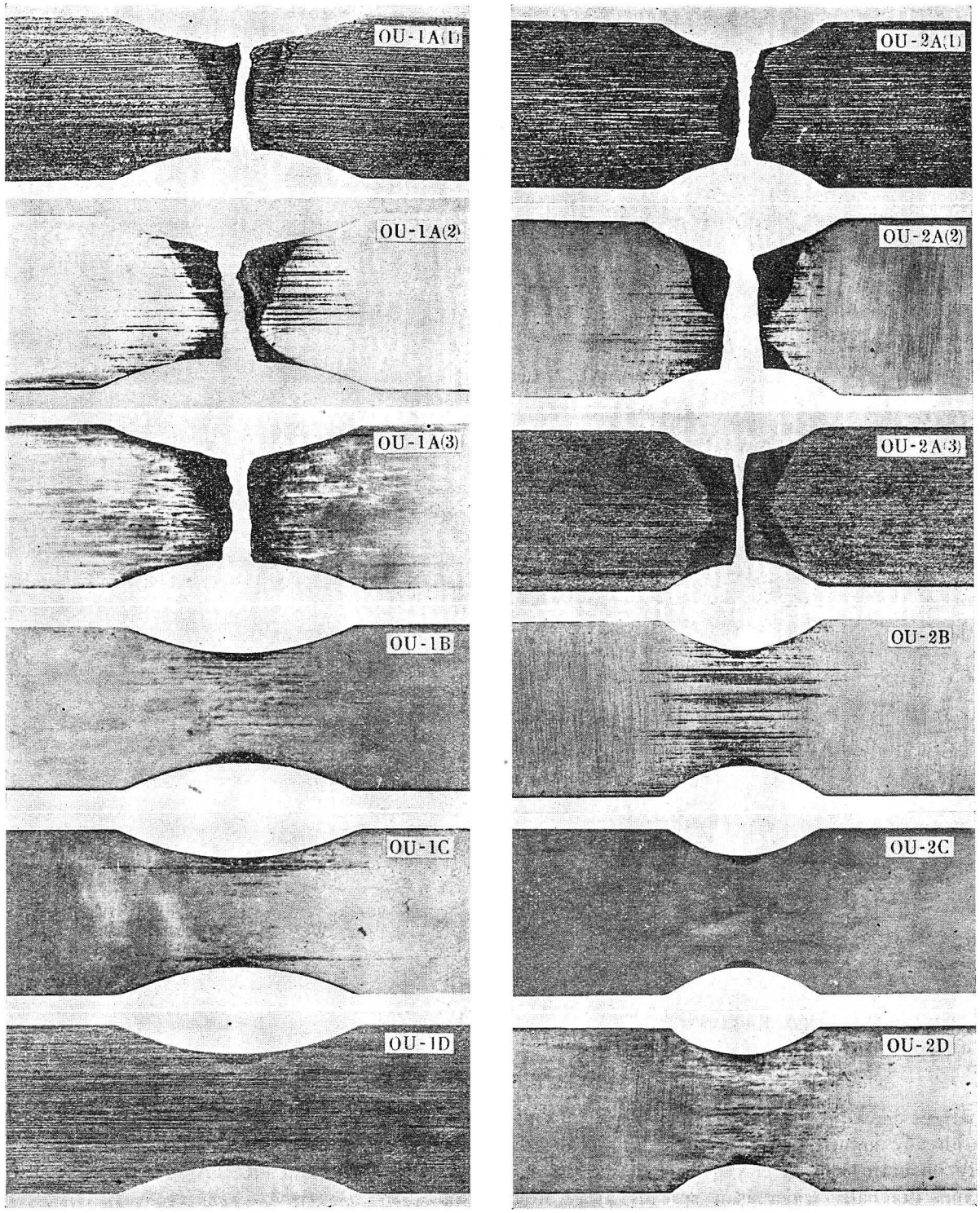

(1) R=23 mm (2) R=10 mm

Fig. 32 (1).

Etching Figures on Specimens in Experiment–2.

the shape of the fatigued zone is very different from that in the preceding paragraph. Let us consider the reason. The specimen with a large fillet radius is considered to be identical to the specimen with smooth surface. Therefore, when the fillet radius is large, the fatigue crack grows very rapidly if it appears at all. Consequently in smooth specimens the fatigue crack has its origin in one point on the circumference of the specimen, while in notched specimens the origins of fatigue cracks exist in every point at the bottom of the notches. So that in smooth specimens the fatigue crack progresses in the shape of a lens having its origin in the middle point of one side, while in notched specimens

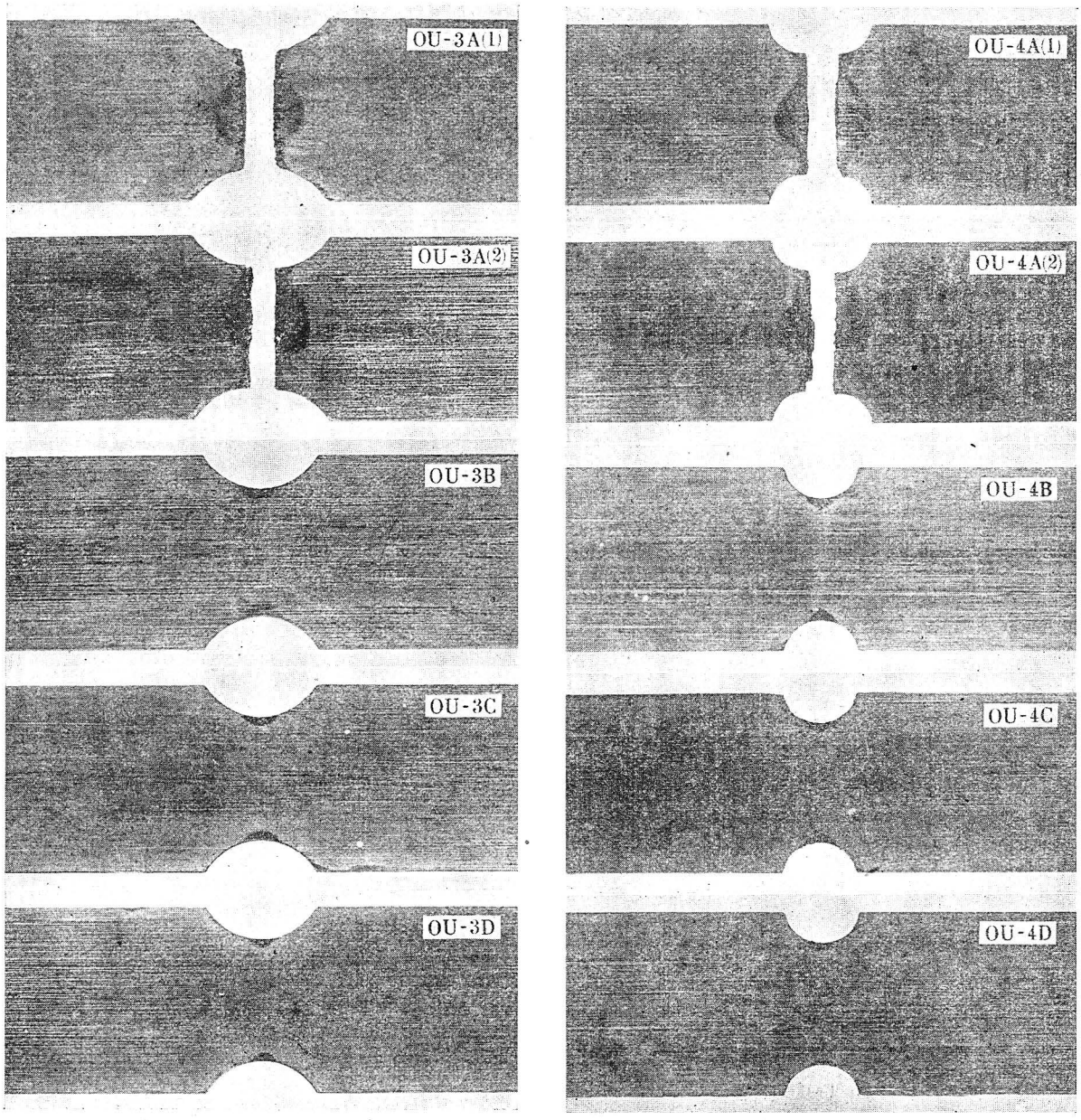

(3) R=5 mm (4) R=3.27 mm

Fig. 32 (2).

Etching Figures on Specimens in Experiment–2.

the fatigue crack progresses in a ring shape. While it is already known that the fatigued zone appears thinly on both sides of cracks near the origin, and becomes gradually wider as it spreads away from the origin.

(α) Therefore, if we take the section of the specimen through the origin, the fatigued zone should appear in a V-shape. Specimen OU–1A(3) shows nearly that shape.

(β) If we take the section of the specimen perpendicular to the above-mentioned section, the fatigued zone should appear in an X-shape. Specimen OU–2A(3) shows that shape.

(γ) If we take the section of the specimen inclined to the above sections, the fatigued zone should appear in an X-shape, the narrowest part of which is not at the center of the specimen. Specimen OU–1A(1) and OU–1A(2) show that shape.

(c) Distinction of notched and unnotched specimens.

As above mentioned, when the fillet radius R is less than 10 mm, the fatigue crack develops uniformly from the circumference, and when the fillet radius R is more than 10 mm, the fatigue crack progresses from one point on the circumference. While, when the fillet radius is equal to 10 mm, the shape of the fatigued zone of specimen OU–2A(1) corresponds to the case of the former, and shapes of fatigued zones of specimens OU–3A(2)

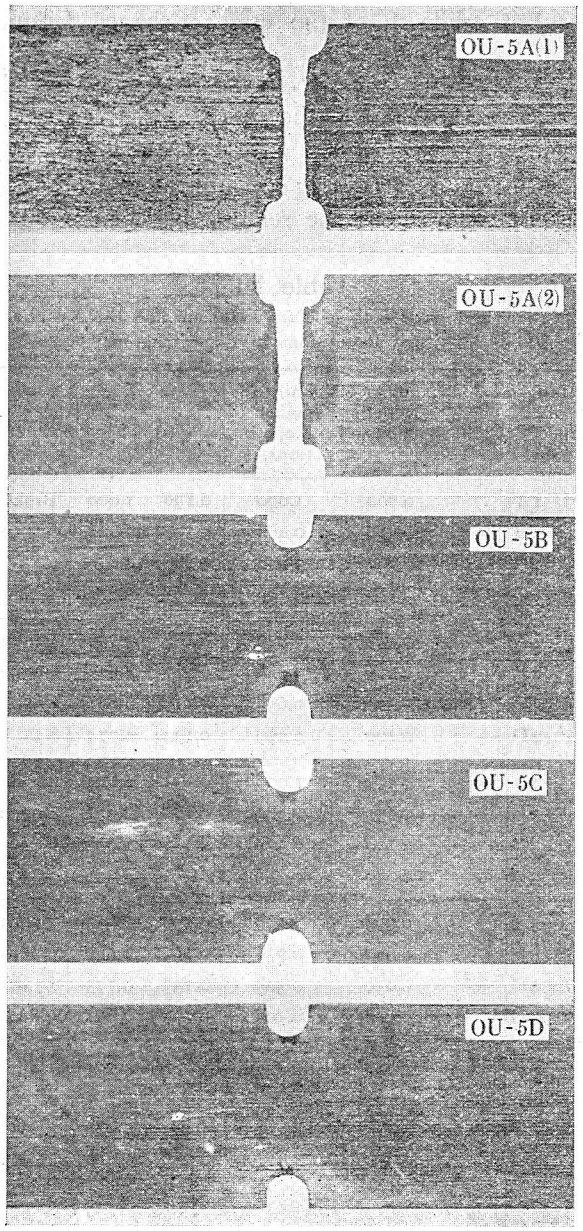

R=1.68 mm

Fig. 32 (3).
Etching Figures in Experiment-2.

and OU-2A(3) correspond to the case of the latter. Therefore, we can regard the case when the fillet radius is equal to 10 mm as the boundary of notched and unnotched cases. That is, the boundary case corresponds to the case when the fillet radius is equal to the diameter of the specimen at the bottom of the notch. It is a well-known fact that the coefficient of notch effect for fatigue in specimens with a fillet radius which is equal to the diameter of the specimen is very small, that is, nearly equal to 1. We must pay attention to the fact that the figure of the fatigued zone shows the characteristics of the specimen with notches, even when the notch effect is thus very small.

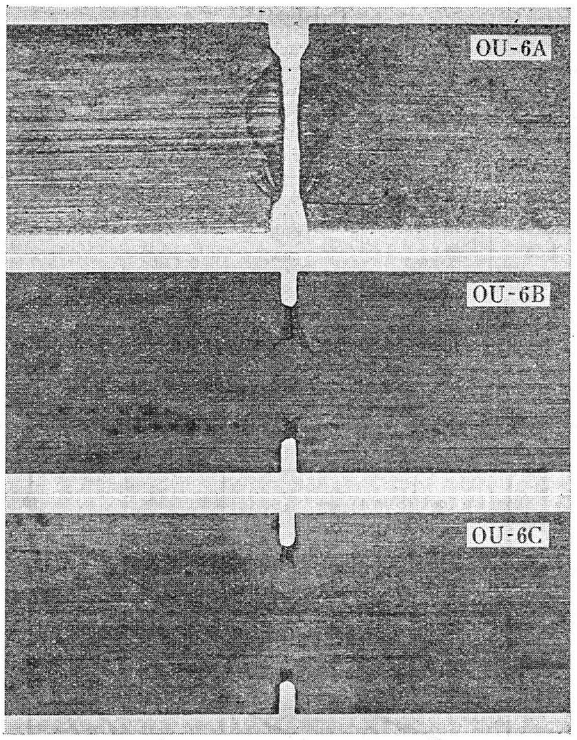

R=0.6 mm

Fig. 32 (4).
Etching Figures in Experiment-2.

(d) Conditions of development of a fatigue crack with relation to the fillet radius.

Let us consider the relation between the number of stress repetitions and the depth of the fatigue crack in the specimen on the process of fatigue. But there is no necessity for considering a case in which the fillet radius is more than 10 mm, because that case is identical with that of a smooth specimen. In a smooth specimen destruction occurs as soon as a fatigue crack appears. So we have considered only cases in which the fillet radius is less than 10 mm.

Let b=depth of the fatigue crack in the specimen on process of fatigue.
r=radius of the specimen at the bottom of the notch.

As the value of b, we took the mean of two values which are obtained for each specimen in Fig. 32. Calculated values of b/r are shown in Table 15. We determined the values of b for broken specimens in the following manner. That is, descriminating the smooth part and the rough part on the fracture of a broken specimen as previously shown in Fig. 26, we took the mean depth of the smooth part as the value of b, which was nearly constant for every broken specimen.

Fig. 33 shows the relation between the number of stress repetitions and depth of the fatigue crack in the specimen in process of fatigue. Points in

Table 15.

Depth of Fatigue Cracks in Experiment-2.

Fillet Radius R, mm	Number of Repetitions, N in 10^6	Ratio of Number of Repetitions, ξ	b/r	Remarks
1.68	0.0347	1.000	0.530	Broken
	0.030	0.865	0.218	Stopped
	0.020	0.577	0.114	,,
	0.010	0.289	0.049	,,
0.60	0.0225	1.000	0.530	Broken
	0.0170	0.756	0.354	Stopped
	0.0113	0.502	0.174	,,

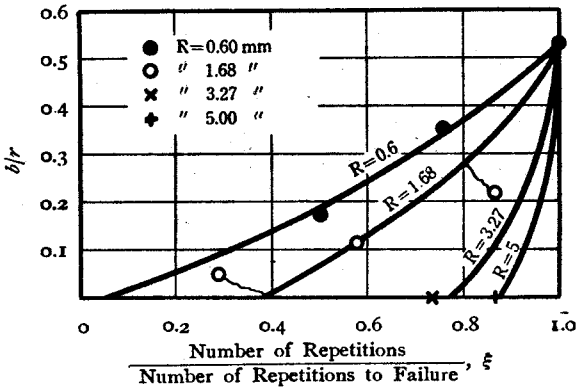

Fig. 33.

Condition of Progression of Fatigue Cracks for Various Fillet Radii.

Fig. 33 are plotted from results of experiments, and curves in Fig. 33 are drawn from the authors' deductions from experimental results. As represented by these curves, we can see that a fatigue crack appears early and grows gradually as the fillet radius becomes smaller. But it must be noted that the number of stress repetitions which is required to break down a specimen after a crack appears is independent of the form of the specimen or the fillet radius. According to results of calculation, the number of stress repetitions to failure from appearance of a crack is about 0.214×10^6 for every specimen.

(e) Relation between depth of the fatigued zone and the number of stress repetitions.

In the specimen with a comparatively large fillet radius, the crescent-shaped fatigued zone appears in early stages of the fatigue process, though the fatigue crack appears only a little before destruction. Then let us consider the relation between the depth of the fatigued zone and the number of stress repetitions applied. Of course the cresent-shaped fatigued zone is essentially the same as the fatigued zone of a smooth specimen. Therefore, the condition of progression of the crescent-shaped fatigued zone must be analogous to that in Fig. 15 and 16.

Let a=depth of the crescent-shaped fatigued zone

r=the radius of the specimen at the bottom of the notch

Calculated values of a/r for specimens with a fillet radius of more than 3.27 mm are shown in Table 16. Fig. 34 shows the relation between a/r and

Table 16.

Relation between Depth of Fatigued Zone and the Number of Stress Repetitions in Experiment-2.

Mark of Specimen	Fillet Radius, R, mm	Number of Repetitions, N in 10^6	Ratio of Number of Repetitions, ξ	a/r	Ratio of a/r, η	Remarks
OU-1A	23	0.602	1.000	0.196	1.000	Broken
,, 1B		0.300	0.498	0.197	1.005	Stopped
,, 1C		0.200	0.332	0.166	0.847	,,
,, 1D		0.100	0.166	0.164	0.837	,,
OU-2A	10	0.335	1.000	0.173	1.000	Broken
,, 2B		0.310	0.926	0.177	1.023	Stopped
,, 2C		0.220	0.657	0.149	0.861	,,
,, 2D		0.100	0.299	0.134	0.775	,,
OU-3A	5	0.173	1.000	0.183	1.000	Broken
,, 3B		0.150	0.867	0.185	1.011	Stopped
,, 3C		0.100	0.578	0.166	0.907	,,
,, 3D		0.050	0.289	0.150	0.820	,,
OU-4A	3.27	0.0952	1.000	0.198	1.000	Broken
,, 4B		0.070	0.736	0.194	0.980	Stopped
,, 4C		0.050	0.525	0.153	0.773	,,
,, 4D		0.010	0.105	0.127	0.641	,,

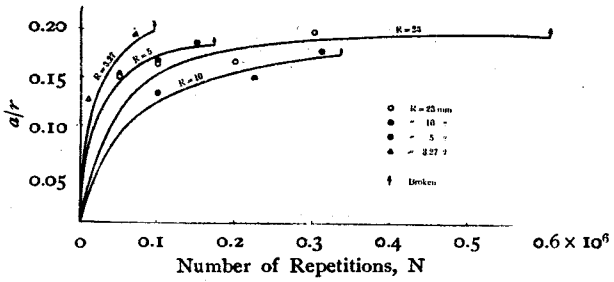

Fig. 34.

Relation between Depth of Fatigued Zone and Number of Repetitions in Experiment-2.

the number of stress repetitions in a diagram. The conditions of progression of the fatigued zone are represented by the curves shown in Fig. 34. In Table 16, the value of a/r for a broken specimen was deduced from the curve in Fig. 34. Let ξ and η represent the same meaning as previously in IV, 2, (b), then values of ξ and η for each specimen are added in Table 16. The relation between ξ and η is shown in Fig. 35. As seen in this figure, the results of the experiments are in good accordance with Equation (1).

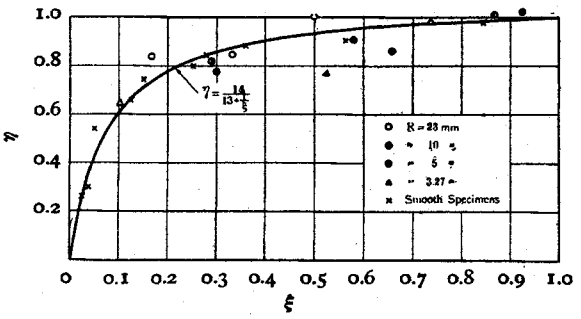

Fig. 35.
Relation between ξ and η.

3. *Experiment–3: Rotating Bending Tests on Specimens with a V-shaped Notch.*

Because in Experiment–2 the applied stress was always equal to 26 kg/mm², the number of stress repetitions to fracture is very small as the fillet radius becomes smaller. For example, when the fillet radius is 0.6 mm, the specimen was broken at 0.0225×10^6 stress repetitions; that is, about 11 minutes of driving time, since the testing machine was driven at about 2000 rev./min. Of course, the applied stress in this case was far more than the yielding point. But we wanted to know about cases in which the applied cyclical stress is a little more than the fatigue limit. So in Experiment–3 we attempted to ascertain the effect of magnitude of cyclical stress applied.

In Experiment–3, the shape of the notch was altered to the V-shape with an angle of 60 degrees, because with the U-shaped notch of a small fillet radius, as in Fig. 29 (6), it was difficult to finish many specimens accurately in the same dimensions. Fig. 36 shows the form and dimensions of the specimens used in Experiment–3.

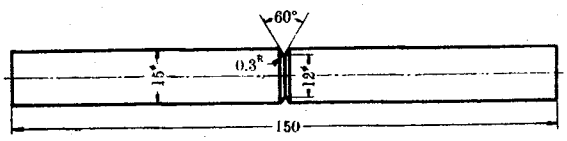

Fig. 36.
Specimen used in Experiment–3.

Results of fatigue tests are shown in Table 17. The fatigue limit was 8.5 kg/mm². Corrosion tests were made on stopped specimens which were fatigued at stresses of 15, 10 and 9 kg/mm²: that is, 76.5, 17.6 and 5.9 per cent more than the fatigue limit, respectively. The number of stress repetitions applied to stopped specimens was decided to be 80 per cent of stress repetitions to failure in every case, because it is not the object of Experiment–3 to ascertain the conditions of progression of a fatigue crack under a definite stress. For specimens which were not broken at stresses less than the fatigue limit, we applied a sufficient number of stress repetitions; that is, more than 10^8, with the intention of making the fatigue crack as large as possible, if it appears at all. Fig. 37 is the stress-endurance diagram which is drawn from the results in Table 17.

Table 17.
Results of Fatigue Tests in Experiment–3.

Mark of Specimen	Maximum Bending Stress, σ kg/mm²	Number of Repetitions, N in 10^6	Remarks
OV–1A	15	0.623	Broken
„ 1B	„	0.498	Stopped
„ 2	11	3.427	Broken
„ 3A	10	5.496	„
„ 3B	„	4.400	Stopped
„ 4A	9	12.859	Broken
„ 4B	„	10.287	Stopped
„ 5	8.5	103.846	Unbroken (Fatigue Limit)
„ 6	8	105.802	Unbroken
„ 7	7	110.569	„

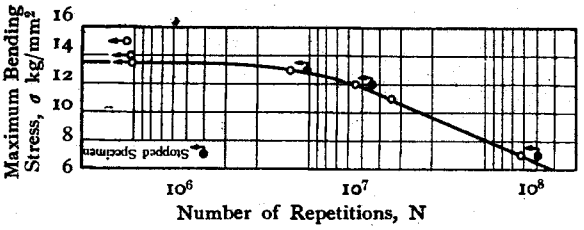

Fig. 37.
Stress-Endurance Curve for Experiment–3.

The material used in Experiment–3 was the same as that in Experiment–2. Therefore, the results of fatigue tests for specimens with a smooth surface were shown in Table 13 and Fig. 30, that is, the fatigue limit is 22.5 kg/mm². So that the coefficient of notch effect for fatigue β becomes as follows:

$$\beta = \frac{22.5}{8.5} = 2.65$$

Photographs of etching figures detected on sections of specimens are shown in Fig. 38. Let us consider these etching figures.

(a) Shapes of fatigued zones.

Shapes of fatigued zones in broken specimens are similar to those obtained at low stresses in Experiment–1, or at a small fillet radius in Experiment–2. In specimen OV–2, the fatigued zone appears narrowly all over the broken section, which is similar to specimen O3U–8 in Experiment–1. We are aware that in Experiment–3 the fatigued zone appears very thinly on both sides of cracks near the bottom of the notches, as seen in specimen

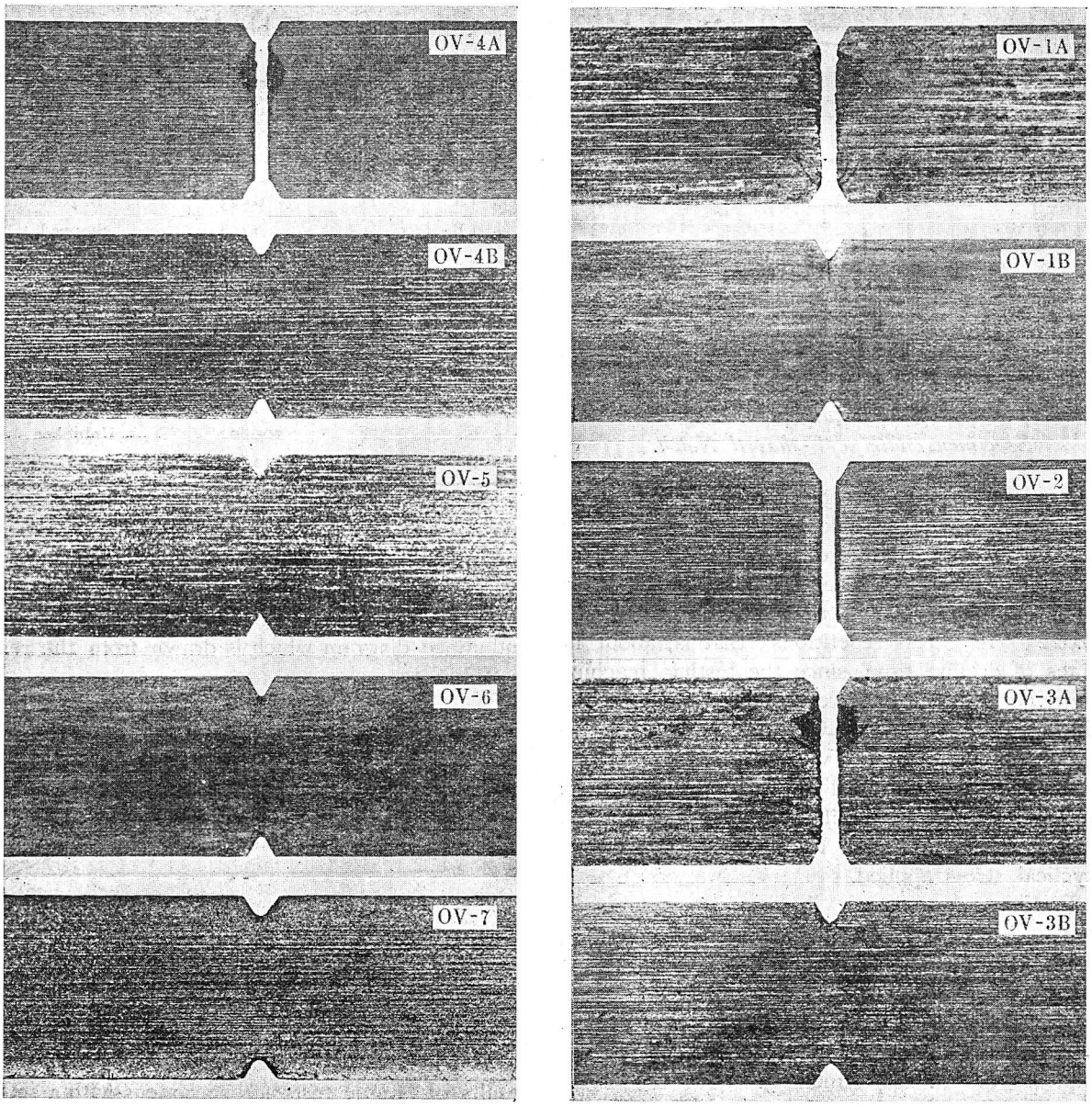

Fig. 38.
Etching Figures on Specimens in Experiment–3.

OV–1A. Also we can scarcely find a fatigued zone in specimen OV–1B. The reason lies perhaps in the fact that the high stressed part in a V-shaped notch is limited to a very narrow zone in comparison with those in U-shaped notches.

(b) Effect of magnitude of stresses upon the condition of progression of fatigue cracks.

In specimen OV–1B, the fatigue crack appears noticeably deep, though the fatigued zone cannot be found at all. Also in specimen OV–3B, the fatigue crack is detected surely, though it is very small in depth and not accompanied with the fatigued zone. And in specimen OV–4B there appears no fatigue crack and also no fatigued zone. Measuring the depth of fatigue crack b and the radius of the specimen r on those stopped specimens, values of b/r were calculated as in Experiment–1 and –2. The results are shown in Table 18. The relations between b/r and the magnitude of the

Table 18.
Depth of Fatigue Cracks in Experiment–3.

Mark of Specimen	Maximum Bending Stress, σ kg/mm²	Maximum Bending Stress / Fatigue Limit	b/r	Remarks
OV–1B	15	1.765	0.193	Stopped
„ 3B	10	1.176	0.072	„
„ 4B	9	1.059	0	„
„ 5	8.5	1.000	0.051	Unbroken (Fatigue Limit)
„ 6	8	0.941	0.091	Unbroken
„ 7	7	0.824	0	„

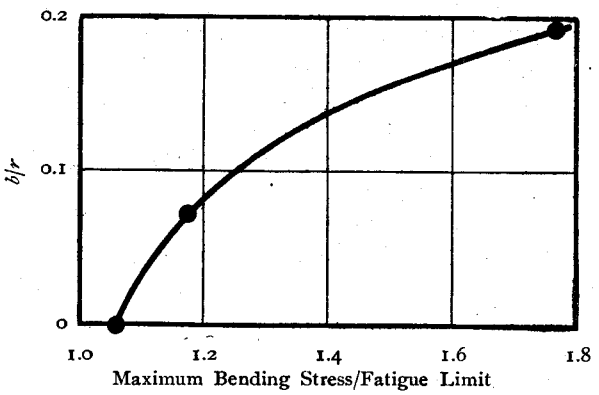

Fig. 39.
Relation between Depth of Cracks and Magnitude of Stress in Experiment-3.

applied stress for stopped specimens are shown in Fig. 39, which is analogous to Fig. 27 in Experiment-1.

From these results we can see the effect of magnitude of stresses upon the development of fatigue cracks. That is, the fatigue crack appears later and grows rapidly as the applied stress becomes lower. But we can never conclude that the number of stress repetitions which is required to break down a specimen after a crack has appeared becomes smaller as the applied stress becomes lower, because specimens OV-1B, OV-3B and OV-4B are considered to be at 0.125×10^6, 1.096×10^6 and 2.572×10^6 stress repetitions respectively before destruction. On the contrary, the authors rather suppose that the number of stress repetitions from the appearance of a fatigue crack to failure becomes larger as the applied stress becomes lower.

(c) About specimens not broken at stresses less than the fatigue limit.

Observing etching figures of three specimens which were not broken at more than 10^8 stress repetitions under the fatigue limit, we can definitely find fatigue cracks in specimens OV-5 and OV-6, though small. But in specimen OV-7 we can find no fatigue crack. The values of b/r for these specimens are added in Table 18. This is very different from the results in Experiment-1 that the fatigue crack appears even in specimens which are not broken at stresses less than the fatigue limit. This problem we shall fully discuss later, in Experiment-4.

4. Experiment-4: Rotating Bending Tests on Specimens with a Deep and Sharp V-shaped Notch.

Let us consider why fatigue cracks appeared in Experiment-3 in unbroken specimens under the fatigue limit and why none appeared in Experiment-1. Considering that the appearance of a fatigue crack in an unbroken specimen is a characteristic of a notched specimen, and that the coefficient of notch effect in Experiment-3 was greater than that in Experiment-1, we may suppose that larger cracks will be detected more clearly in unbroken specimens under a fatigue limit, if the experiments are made on specimens with a larger notch effect than in Experiment-3. From this supposition, we made experiments on specimens with a deep and sharp V-shaped notch. The form and dimensions of the specimen used in Experiment-4 are shown in Fig. 40. The notch is V-shape with an angle of 60 degrees, and the fillet radius at the bottom of the notch was made as small as possible, so far as uniformity permitted.

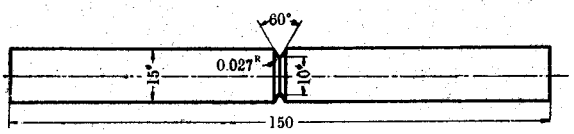

Fig. 40.
Specimen used in Experiment-4.

Table 19.
Results of Fatigue Tests in Experiment-4.

Mark of Specimen	Maximum Bending Stress, σ kg/mm^2	Number of Repetitions, N in 10^6	Remarks
ODV-1	10	2.013	Broken
ODV-2	8	2.387	„
ODV-3	5	4.804	„
ODV-4	3	75.570	Unbroken (Fatigue Limit)
ODV-5	2	30.027	Unbroken

Results of fatigue tests are shown in Table 19. The fatigue limit was 3 kg/mm^2. For unbroken specimens under the fatigue limit we intended to apply a sufficiently large number of stress repetitions, but it was not so large as in Experiment-3. In Experiment-4 we made no test on a stopped specimen above the fatigue limit. Fig. 41 shows the stress-endurance diagram.

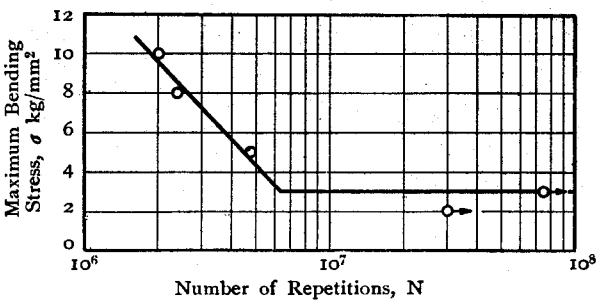

Fig. 41.
Stress-Endurance Curve for Experiment-4.

The material used in Experiment-4 was the

same as that in Experiment–2. Therefore, the fatigue limit of smooth specimens for the material is 22.5 kg/mm², as previously mentioned in Table 13 and Fig. 30. So that the coefficient of notch effect for fatigue β is as follows:

$$\beta=\frac{22.5}{3}=7.5$$

Photographs of etching figures detected on sections of specimens are shown in Fig. 42. Considerations drawn from these etching figures are as follows:

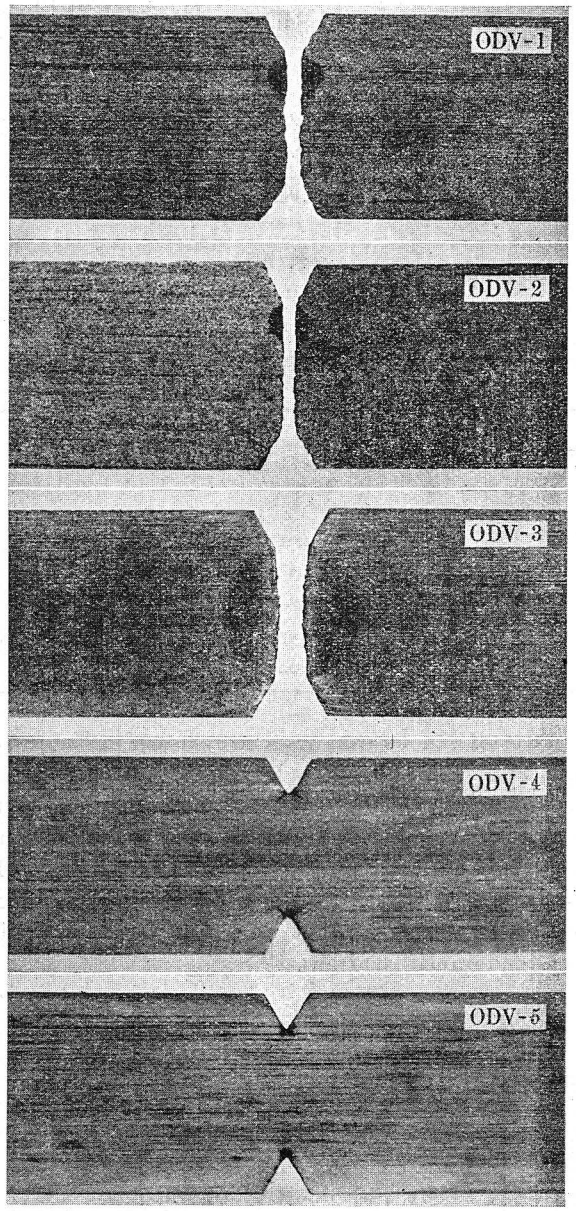

Fig. 42.
Etching Figures on Specimens in Experiment–4.

(a) Fatigued zones and fatigue cracks.

Fatigued zones in specimens ODV–1 and ODV–2 are quite similar to those in Experiment–3. It can be clearly seen in these specimens that the wide part of the fatigued zone becomes smaller as the applied stress diminishes. But in specimen ODV–3 the fatigued zone appears in a singular shape which has not been found before; that is, in a round shape over the whole section. The authors consider the round shaped fatigued zone as an extraordinary figure.

In specimens ODV–4 and ODV–5, which were not broken under the fatigue limit, fatigue cracks are clearly found. In specimen ODV–4, fatigue cracks appear in two branches in directions inclined at about 45 degrees to the longitudinal axis of the specimen, which the authors consider also as an extraordinary result. In specimen ODV–5, the fatigue cracks are of the ordinary appearance.

(b) Fatigue cracks in specimens not broken under the fatigue limit.

It is in accordance with the authors expectations that fatigue cracks can be detected in specimens subjected to stresses far less than the fatigue limit. The relation between the coefficient of notch effect and the smallest stress required to generate a fatigue crack in Experiments–1, 3 and 4 is as follows:

Experiment–1.....β=1.99 and γ=1.00
„ 2.....„ 2.65 „ „ 0.94
„ 3.....„ 7.5 „ „ 0.67

where β=coefficient of notch effect for fatigue

$$\gamma=\frac{\left(\begin{array}{c}\text{the smallest stress required to generate}\\ \text{a fatigue crack}\end{array}\right)}{\text{fatigue limit}}$$

As seen in the above Table, the smallest stress required to generate a fatigue crack becomes lower as the coefficient of noch effect increases.

At what time does the fatigue crack appear? Is the fatigue crack progressive? We do not know. But it is sure, at least, that the crack did not appear in the early stage of the fatigue process, because we have already known that the fatigue crack appears later and grows rapidly as the applied stress becomes lower. We must pay attention to the fact that the meaning of the fatigue limit becomes vague, if the crack is progressive. But even if the crack is progressive, its rate of growth must become smaller suddenly at the fatigue limit, because the stress-endurance curve bends sharply at the fatigue limit.

5. *Experiment–5: Reversed Torsinal Tests on Specimens with a V-shaped Notch.*

All fatigue tests in Experiment–1 to 4 were rotating bending tests of uniform bending moment type. In Experiments–5 and 6, we shall consider cases of reversed torsional tests. In torsional tests

the longitudinal notch is desirable, because it has a larger effect than the lateral notch. But we adopted the annular V-shape as the form, because it causes least trouble in accurate machining and measurement, and also in selection of the etching section.

Fig. 43 (1) and (2) show specimens used in the experiment. Fig. 43 (1) is the specimen with a smooth surface, which was used only to obtain the fatigue limit and not subjected to corrosion tests. Test results on the smooth specimen are shown in Table 20. The fatigue limit was 13.5 kg/mm². Fig. 43 (2) is the specimen with a notch.

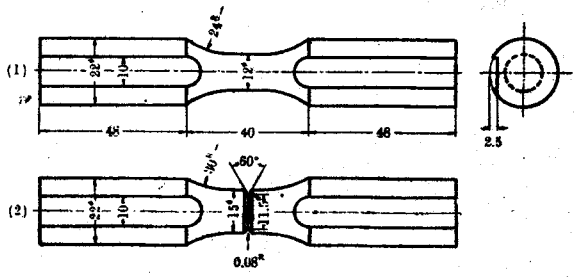

Fig. 43.
Specimens used in Experiment–5.
(1) Smooth Specimen, (2) Notched Specimen.

Table 20.

Results of Fatigue Tests on Smooth Specimens in Experiment–5.

Mark of Specimen	Maximum Torsional Stress, τ kg/mm²	Number of Repetitions, N in 10^6	Remarks
TN–1	15.0	1.725	Broken
„ 2	14.5	4.584	„
„ 3	14.0	3.114	„
„ 4	13.5	10.026	Unbroken (Fatigue Limit)

Table 21.

Results of Fatigue Tests on Notched Specimens in Experiment–5.

Mark of Specimen	Maximum Torsional Stress, τ kg/mm²	Number of Repetitions, N in 10^6	Remarks
TV–1	17.0	0.0110	Broken
„ 2	15.0	0.0102	„
„ 3	13.0	0.0396	„
„ 4A	12.0	0.0430	„
„ 4B	„	0.0344	Stopped
„ 5A	11.0	0.0501	Broken
„ 5B	„	0.0401	Stopped
„ 6	10.0	0.0860	Broken
„ 7	9.0	0.1652	„
„ 8	8.0	0.3821	„
„ 9A	7.5	0.5048	„
„ 9B	„	0.4038	Stopped
„ 10	7.0	10.6006	Unbroken (Fatigue Limit)

Test results on the notched specimens are shown in Table 21. The fatigue limit was 7 kg/mm². Corrosion tests were made on stopped specimens on the way to failure, which were fatigued at cyclical stresses of 12, 11 and 7.5 kg/mm²; that is, 71.4, 57.1 and 7.1 per cent over the fatigue limit, respectively. Numbers of stress repetitions applied to those stopped specimens were always equal to 80 per cent of the stress repetitions to failure, as in Experiment–3. Fig. 44 shows stress-endurance

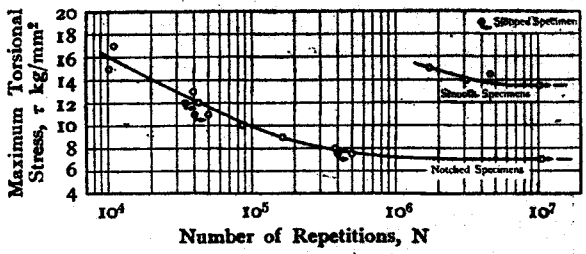

Fig. 44.
Stress-Endurance Curves for Experiment–5.

curves drawn from Table 20 and Table 21. The coefficient of notch effect for fatigue β in this case is as follows:

$$\beta = \frac{13.5}{7} = 1.93$$

Photographs of etching figures detected on notched specimens are shown in Fig. 45. Considerations drawn from these etching figures are as follows:

(a) About broken specimens.

It is observed in Fig. 45 that five specimens broken at stresses more than 11 kg/mm²; i.e., from TV–1 to TV–5A, are not separated into two pieces, though four broken specimens less than 10 kg/mm², i.e., from TV–6 to TV–9A, are completely separated. The reason can be explained by the following consideration. The fatigue testing machine used in this experiment was Nishihara's repeated torsion machine. The testing machine has the following construction: one side of the specimen is attached to a fly wheel and forced vibration is transmitted to the fly wheel from the other side of the specimen by a crank and eccentric mechanism. Thus the inertia force of the fly wheel due to vibration exerts torsional moment on the specimen. The amplitude of the fly wheel must be kept at a constant value for a certain specimen from the beginning of the test to destruction. But when a crack appears in a specimen, the natural vibration frequency of the specimen decreases suddenly. So that we cannot vibrate the fly wheel with a large amplitude, when the crack grows to some extent. Therefore we must stop the test before the specimen breaks down into two pieces, if the stress applied

to the specimen is large. Thus we regarded the specimen in which a crack had grown to some extent as approximately a broken specimen. But there must occur little error in the approximation, because fatigue cracks in specimens TV–1 to TV–5 are very deep, as seen in Fig. 45.

(b) About fatigue cracks.

The fatigue crack progresses in a radial direction, as in the case of rotating bending tests. But the path of the crack in a torsional specimen

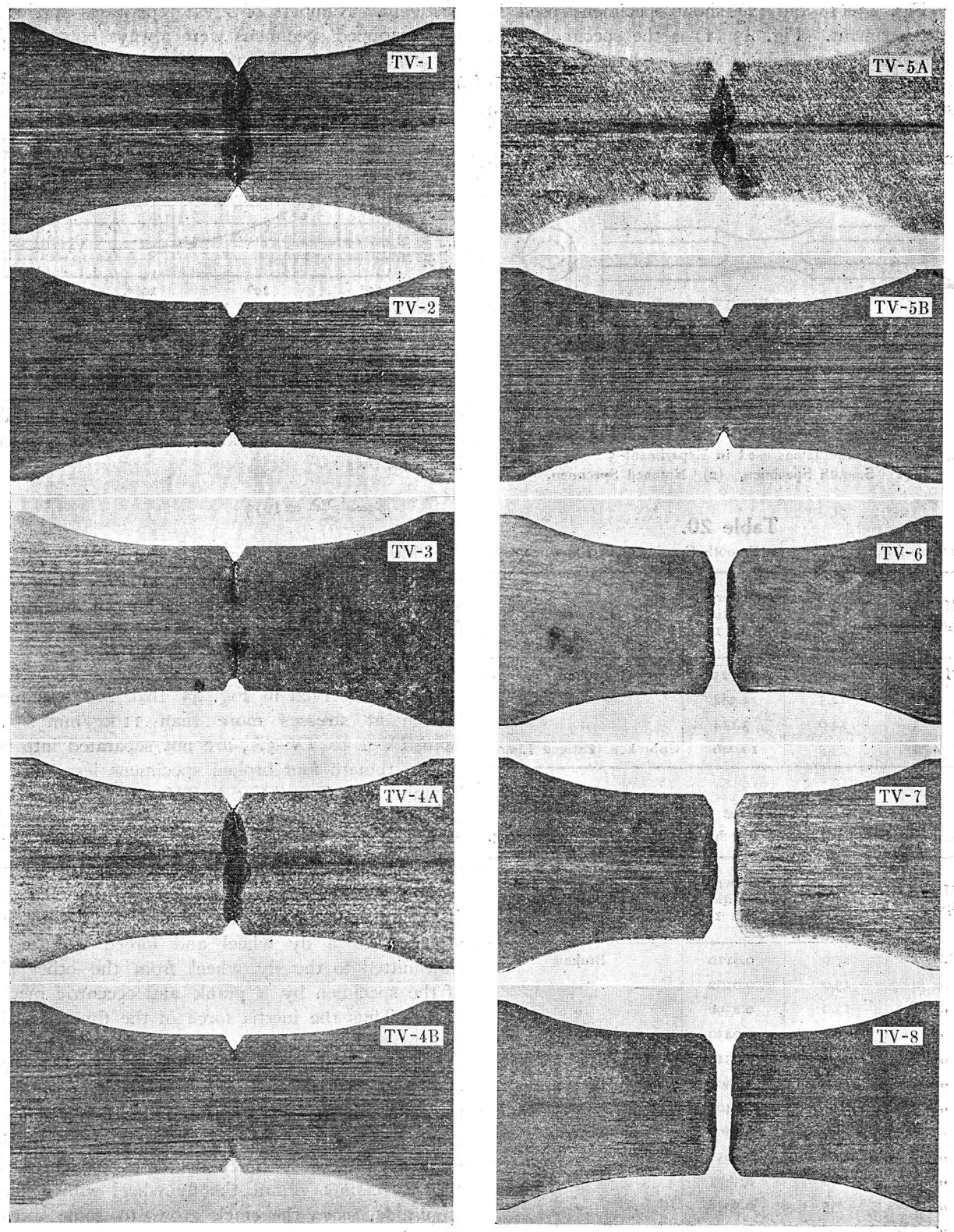

Fig. 45 (1).
Etching Figures on Specimens in Experiment–5.

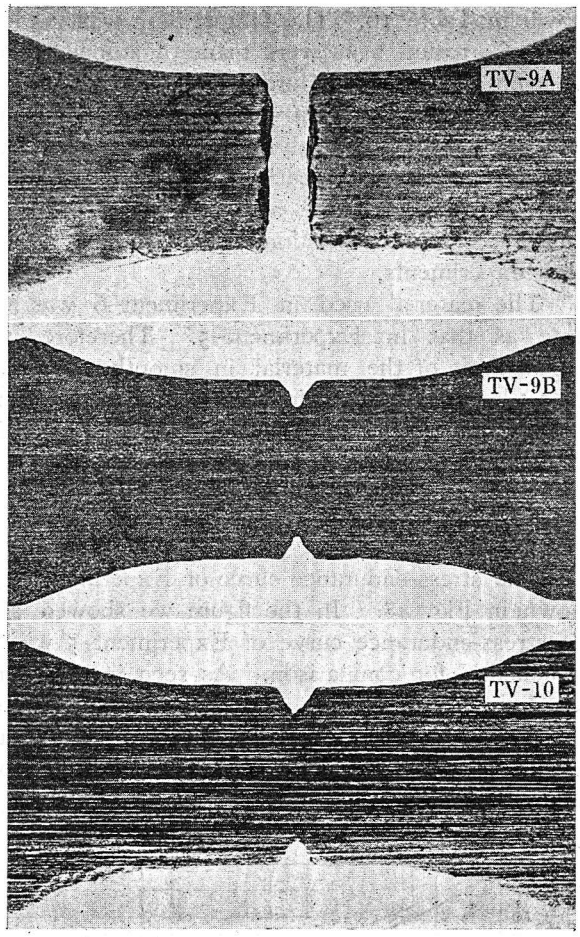

Fig. 45 (2).
Etching Figures on Specimens in Experiment-5.

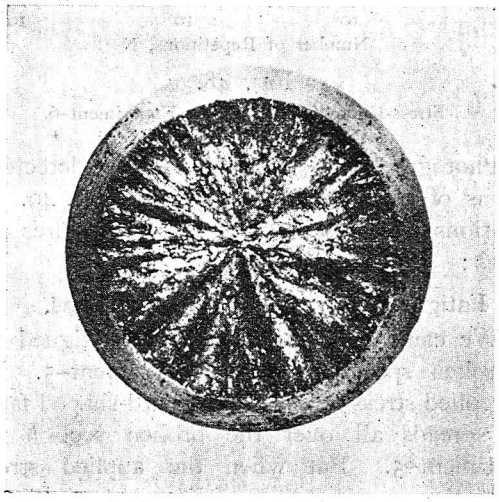

Fig. 46.
Fatigue Fracture of Notched Specimen at Reversed Torsional Test.

is not so smooth as it was in a bending specimen. It can be seen by minute observation that the crack progresses along the radial line with many small windings. Moreover, the crack has a tendency to separate in two branches, as seen in specimens TV-3, TV-4 and TV-7. Let us consider the reason. It is a well-known fact that the fatigue fracture of carbon steel occurs always in the plane of the maximum principal stress. In a torsional specimen the plane of the maximum principal stress has the angle of about 45 degrees to the cross section of the specimen. Therefore the torsional specimen cannot be broken at a cross section through the bottom of the notch. The torsional fatigue fracture of a notched specimen generally shows a ragged surface with many radial creases, as shown in Fig. 46, for example. From these considerations we can easily understand the reason why the fatigue crack winds and has a tendency to separate in two branches.

(c) About fatigued zones.

The fatigued zone on a broken specimen appears narrowly at the bottom of the notch and becomes gradually wider towards the center of the specimen, as was the case in bending specimens. But in torsional specimens the fatigued zone becomes narrow once again near the center of the specimen. Consequently the fatigued zone generally takes the shape of a gourd. The reason can be explained as follows: We already know that the fatigued zone spreads in the direction of the maximum shear stress. Now in a torsional specimen the direction of the maximum shear stress is in the plane perpendicular to the longitudinal axis of the specimen. Therefore the figure of the fatigued zone spreads in a radial direction and has no tendency to become wider. The fatigued zone appears narrow at the smooth part of fracture, and wide at the ragged part. As previously mentioned, concerning Fig. 46, the surface of a fatigue fracture is comparatively smooth at the central part of the specimen, because all radial creases converge on the center of the specimen. Accordingly we can understand the reason why the fatigued zone is narrowest at the central part of a torsional specimen.

We can also see in Fig. 45 that the gourd-shaped fatigued zone appears wider in the high stressed specimen than in the low stressed specimen. The reason can be explained by the fact that fracture of broken specimens is more ragged in the high stressed specimen than in the low stressed specimen.

(d) About stopped and unbroken specimens.

In the stopped specimen TV-4B, slight fatigue cracks are detected at the bottoms of the notches. And the fatigued zone appears nearly in an elliptical shape, surrounding the fatigue cracks. That is, the shape of the fatigued zone in torsional specimens is very different from that in bending specimens. In the stopped specimen TV-5B, we cannot find fatigue cracks, but there appear fatigued zones which progress radially in many lines from

the bottoms of the notches. In the stopped specimen TV–9B, we cannot find either fatigue cracks or fatigued zones. But after applying the specimen to a corrosion test for a long time, it showed a shape which was scraped out at the bottoms of notches, as seen in Fig. 45. The reason is perhaps that there exist also damaged parts at the bottoms of notches, and these parts were melted and disappeared more rapidly than the other parts.

From these stopped specimens it can be deduced that the fatigue crack appears later and grows rapidly as the applied stress becomes lower; similar to the case of rotating bending.

In the specimen TV–10, which was not broken at the stress under the fatigue limit, we found also slight damaged parts at the bottoms of the notches after a long corrosion time.

Table 22.

Results of Fatigue Tests in Experiment–6.

Mark of Specimen	Maximum Torsional Stress, τ kg/mm²	Number of Repetitions, N in 10^6	Remarks
TDV–1A	12	0.032	Broken
„ 1B	„	0.025	Stopped
„ 2	8	0 172	Broken
„ 3	6	1.392	„
„ 4A	5	1.960	„
„ 4B	„	1.568	Stopped
„ 5	4.5	11.435	Unbroken (Fatigue Limit)

6. *Experiment–6: Reversed Torsional Tests on Specimens with a Deep and Sharp V-shaped Notch.*

Specimens TV–4B and TV–5B in Experiment–5 showed fatigue cracks or fatigued zones very slightly, though the specimen was subjected to a comparatively high stress and was in a condition near to destruction. The reason was perhaps the smallness of the value of notch effect in Experiment–5. Therefore in Experiment–6 we made experiments on specimens with a deeper and sharper V-shaped notch.

The form and dimensions of the specimen used is shown in Fig. 47. Results of fatigue tests are

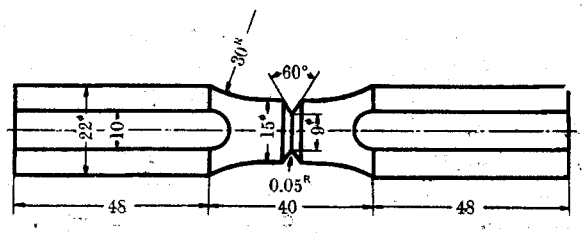

Fig. 47.

Specimen used in Experiment–6.

shown in Table 16. The fatigue limit was 4.5 kg/mm². Corrosion tests were made on stopped specimens on the way to failure, which were fatigued at cyclical stresses of 12 and 5 kg/mm²; i.e., 16.7 and 11.1 per cent respectively over the fatigue limit. Numbers of stress repetitions applied to these stopped specimens were always equal to 80 per cent of the stress repetitions to failure, as in previous experiments.

The material used in Experiment–6 was the same as that in Experiment–5. Therefore, the fatigue limit of the material in smooth specimens is 13.5 kg/mm², as previously mentioned in Table 20 and Fig. 44. The coefficient of notch effect for fatigue β is as follows:

$$\beta = \frac{13.5}{4.5} = 3.0$$

The stress-endurance curve of Experiment–6 is shown in Fig. 48. In the figure we showed also the stress-endurance curve of Experiment–5 with a broken line, for comparison. As seen in the figure, the difference of stress-endurance curves between the cases at high stress parts is comparatively small, though the fatigue limit of Experiment–6 is considerably smaller than that of Experiment–5.

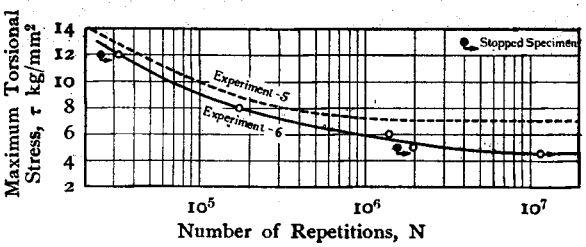

Fig. 48.

Stress-Endurance Curve for Experiment–6.

Photographs of etching figures detected on sections of specimens are shown in Fig. 49. Considerations drawn from these etching figures are as follows:

(a) Fatigued zones of broken specimens.

We can see the gourd-shaped fatigued zones on broken specimens as in Experiment–5. When the applied stress is large, the gourd-shaped fatigued zone spreads all over the broken section as in Experiment–5. But when the applied stress is small, the gourd-shaped fatigued zone becomes small; which is similar to the results in rotating bending tests. Besides the gourd-shaped fatigued zone is not always situated at the center of a specimen, but generally leans to one side. This point is also similar to the results in rotating bending tests.

(b) About stopped and unbroken specimens.

In the stopped specimens TDV–1B, fatigued zones and fatigue cracks were detected to a con-

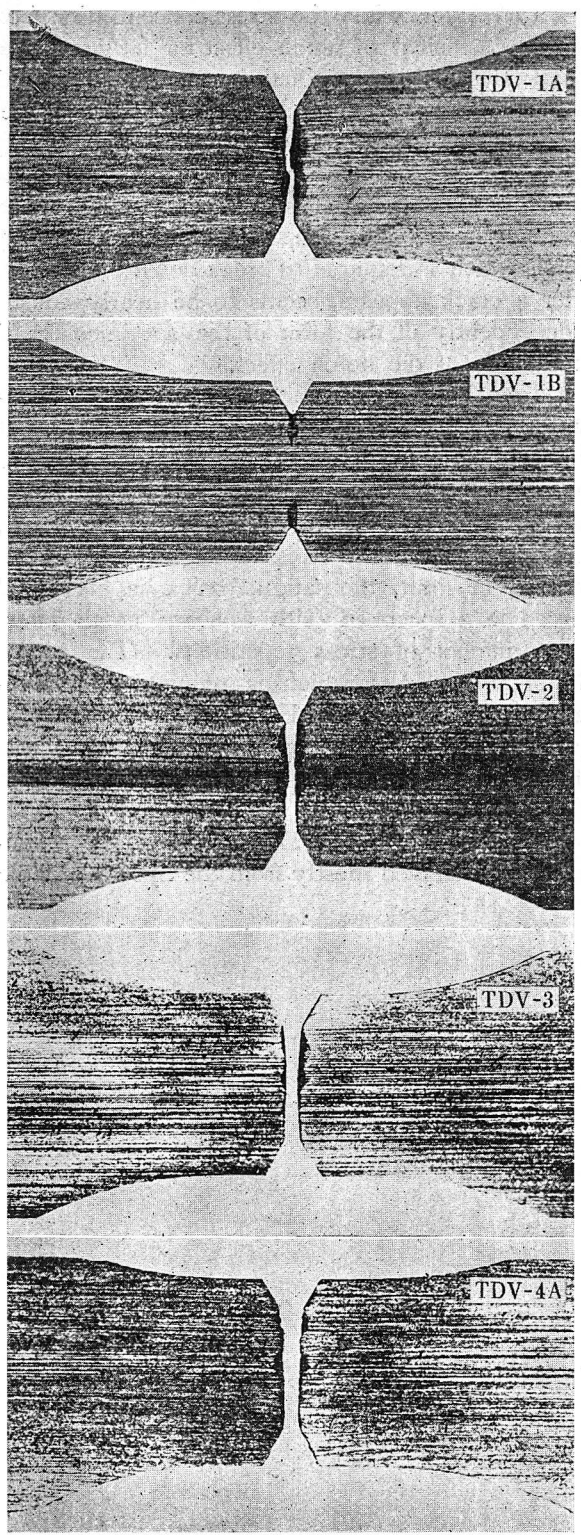

Fig. 49 (1)
Etching Figures in Experiment–6.

siderable extent. The value of b/r in the specimen was about 0.24. Comparing specimen TDV–1B with specimen TV–4B in Experiment–5, we see that the fatigue crack in TDV–1B is very much deeper than in TV–4B. Both specimens had received just 80 percent of stress repetitions to failure,

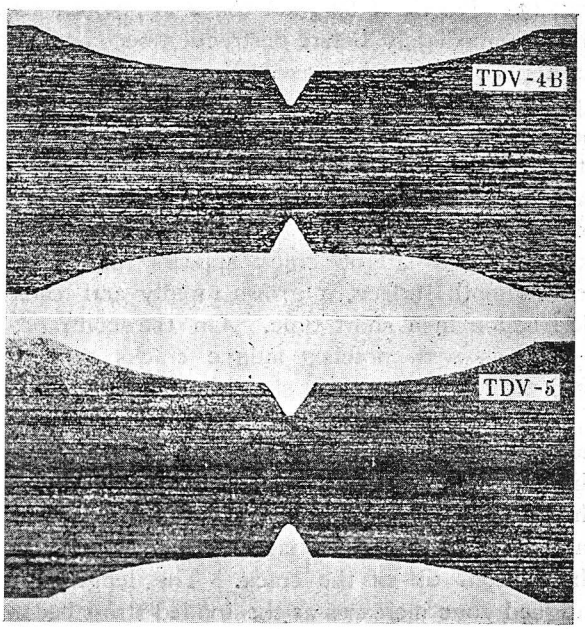

Fig. 49 (2)
Etching Figures in Experiment–6.

besides there is no wide gap in the numbers of stress repetitions to failure in both specimens, as seen in Fig. 48. From these results it can be deduced that a fatigue crack grows more gradually as the notch effect becomes larger. The relation is quite similar to the case of rotating bending tests.

The appearance of the fatigued zone in specimen TDV–1B is very different from that in rotating bending specimens. That is, the fatigued zone spreads along the radial direction, and the depth of the fatigued zone is far greater than the depth of the fatigue crack.

In specimens TDV–4B and TDV–5, we could not find any fatigued zone or fatigue crack at all.

VI. Summary of Results.

Fatigued zones are detected on various specimens by the corrosion method. The important results obtained in this paper are summarized as follows:

(1) Figures of fatigued zones in smooth specimens are very different from the so-called strain figures in static specimens. That is, the fatigued zone appears first at the highest stress parts and develops gradually to lower stress parts.

(2) Development of fatigued zones is rapid at the beginning of stress repetitions and becomes slow gradually. If we represent the number of stress repetitions in ratio to the number of repetitions to failure, the rate of growth of fatigued zones becomes definite independently of kinds of tests and also magnitude of applied stresses.

(3) Depth of fatigued zones in smooth specimens immediately before destruction becomes larger as applied stresses increase. Besides, fatigued zones appear even in specimens which are not broken under the fatigue limit. The ratio of the smallest stress which is required to generate fatigued zones to the the fatigue limit seems to be independent of the kind of tests.

(4) If a fatigue crack appears in specimens with smooth surface, it grows rapidly and leads to destruction in a short time. On the contrary, in specimens with notches fatigue cracks grow and lead to destruction very slowly.

(5) The fatigue crack in specimens with notches progresses in the direction of the plane of the maximum principal stress. On the contrary, the fatigued zone in notched specimens progresses in the direction of the maximum shear stress from the bottom tip of the crack. The length of the fatigued zone increases as the applied stress becomes higher.

(6) In the smooth specimen, the fatigue crack progresses from one point on the surface of the specimen, but in the notched specimen the fatigue crack progresses uniformly from the bottom of the notch. Therefore, the shape of the fatigued zone is different according to whether the specimen has a smooth surface or is notched.

(7) Even when the stress concentration factor or the coefficient of notch effect for fatigue is very small (that is, nearly equal to 1), the figure of the fatigued zone shows the characteristics of specimens with notches.

(8) The fatigue crack appears early and grows gradually as the stress concentration factor becomes large. But the number of stress repetitions, which is required to break down the specimen after a crack appears, seems to be nearly constant independently of the form of the specimen or the magnitude of the notch effect.

(9) The fatigue crack appears later and grows rapidly as the applied stress becomes smaller. But the number of stress repetitions to failure from appearance of a fatigue crack seems to become rather larger as the applied stress becomes smaller.

(10) When the stress is slightly smaller than the fatigue limit, the fatigue crack is clearly observed in a specimen with a sharp notch after a great number of stress repetitions. The ratio of the smallest stress which is required to generate fatigue cracks in notched specimens to the fatigue limit becomes smaller as the coefficient of notch effect becomes larger.

Acknowledgment: The cost of this research has been defrayed mostly from the Syōwa Hōkōkai.